Journal Pre-proofs

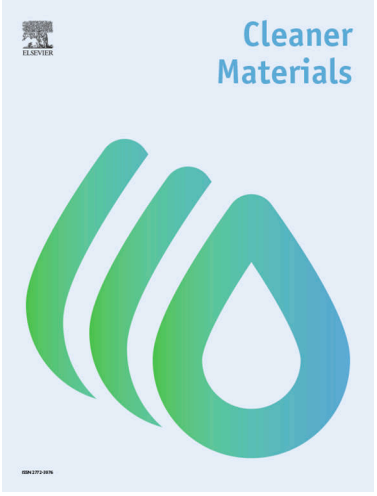

Experimental study of phase change material (PCM) biochar composite for net-zero built environment applications

Mohamed Katish, Stephen Allen, Adam Squires, Veronica Ferrandiz-Mas

PII: S2772-3976(24)00058-3
DOI: https://doi.org/10.1016/j.clema.2024.100274
Reference: CLEMA 100274

To appear in: *Cleaner Materials*

Received Date: 1 June 2024
Revised Date: 16 October 2024
Accepted Date: 16 October 2024

Please cite this article as: M. Katish, S. Allen, A. Squires, V. Ferrandiz-Mas, Experimental study of phase change material (PCM) biochar composite for net-zero built environment applications, *Cleaner Materials* (2024), doi: https://doi.org/10.1016/j.clema.2024.100274

Experimental Study of Phase Change Material (PCM) Biochar Composite for Net-Zero Built Environment Applications

Mohamed Katish[a,b,c], Stephen Allen[b,c], Adam Squires[b,d] and Veronica Ferrandiz-Mas[a,b,c]*

a Centre for Integrated Materials, Processes and Structures, University of Bath, UK
b Institute for Sustainability, University of Bath, UK
c Department of Architecture and Civil Engineering, University of Bath, UK
d Department of Chemistry, University of Bath, UK

Corresponding Author:

Mohamed Katish

Email: mak228@bath.ac.uk

Centre for Integrated Materials, Processes and Structures

University of Bath, Bath, United Kingdom, BA2 7AY

Experimental Study of Phase Change Material (PCM) Biochar Composite for Net-Zero Built Environment Applications

Mohamed Katish[a,b,c], Stephen Allen[b,c], Adam Squires[b,d] and Veronica Ferrandiz-Mas[a,b,c]*

a Centre for Integrated Materials, Processes and Structures, University of Bath, UK
b Institute for Sustainability, University of Bath, UK
c Department of Architecture and Civil Engineering, University of Bath, UK
d Department of Chemistry, University of Bath, UK

Corresponding Author:

Mohamed Katish

Email: mak228@bath.ac.uk

Centre for Integrated Materials, Processes and Structures

University of Bath, Bath, United Kingdom, BA2 7AY

Abstract

This study presents a novel and sustainable method for integrating octadecane phase change material (PCM) into traditional building materials like mortar and gypsum using vacuum-impregnated biochar. Optimising the impregnation conditions resulted in a PCM-biochar composite with 62.21% PCM loading and a latent heat energy of approximately 116.7 J. g^{-1}, as measured by Differential Scanning Calorimetry (DSC). Thermogravimetric Analysis (TGA) confirmed the composite's stability at high temperatures, while accelerated DSC validated its phase change capability and stability over 300 cycles. Characterisation via Scanning Electron Microscopy (SEM), Small-Angle X-ray Scattering (SAXS), X-ray Diffraction (XRD), and Solid-State Proton Nuclear Magnetic Resonance (^{1}H NMR) verifies PCM retention within biochar pores and reveals interactions between PCM and biochar. Additionally, the non-pozzolanic nature of biochar is confirmed. Workability tests show reduced consistency with increased PCM-biochar content in mortar. At 40% sand replacement rate with PCM-biochar, the compressive strength initially decreases by 45.50% after 28 days, but it improves to 43 MPa after 120 days. Gypsum samples retain adequate strength for retrofitting applications (2 MPa), demonstrating the potential of PCM-biochar composites to enhance thermal energy storage in building materials, thereby supporting Net-zero building objectives.

Introduction

Expansion in cities and population growth results in an increased demand for indoor heating and cooling, which increases the carbon dioxide emissions (CO_2e) of the built environment (United Nations Environment Programme, 2022). The built environment is the third largest end use of energy with 74% of gas and electricity having been used for domestic heating in the UK in 2021 (Department for Business, Energy & Industrial Strategy (BEIS), 2022). As reported by the UK *Department for Business, Energy & Industrial Strategy*, the rise in energy consumption is primarily met using fossil fuel-based resources, leading to the release of more CO_2e into the atmosphere (Department for Business, Energy & Industrial Strategy (BEIS), 2022). Recently, a new solution has emerged to lower energy demand for space heating and cooling, and this solution revolves around the inclusion of Phase Change Materials (PCMs) into building materials. PCMs are substances that absorb and release significant amount of thermal energy by changing from one phase to another, such as from solid to liquid or liquid to solid (Pielichowski & Pielichowska, 2014). By utilising the properties of PCM, significant reductions in energy usage and CO_2e can be achieved.

PCMs can be incorporated into various elements of the built environment, including walls, columns, ceilings, floorings, and facades. In cold regions, PCM can store heat during the day, as temperatures drop during the colder periods of the day, the PCM releases the stored heat, assisting in maintaining comfortable indoor temperatures. Similarly, in warm regions, PCM can absorb excess heat during the day, thereby reducing the need for air conditioning and during the cooler periods of the day the PCM releases the stored heat, providing natural cooling effect (Kenisarin, 2014). This thermal energy regulation reduces the dependency on traditional heating and cooling systems, resulting in substantial energy savings and decreased CO_2e. Despite the promising potential of PCM in the built environment, PCM has often been overlooked for several reasons. For instance, Phase Change Materials (PCMs) can be sensitive to environmental conditions, such as moisture, chemicals and physical stress thus hindering their stability and durability overtime (Huang, et al., 2023). Furthermore, PCMs which are suitable for built environment applications, especially in terms of their phase change temperature and their latent heat energy, usually are materials with solid to liquid phase change temperatures thus rising another issue which is leakage and contamination. During phase change, PCMs can leak to the surrounding materials which can affect their structural integrity and performance (Al-Yasiri & Szabó, 2021). Finally, mixing PCMs directly with building materials, such as mortar, can be detrimental to the mortar properties as it has an adverse effect on the interactions within mortar constituents such as hindering the hydration reaction of cement (Eddhahak-Ouni, et al., 2014).

To improve PCMs durability and compatibility with building materials, different methods have been investigated in the literature. These methods, among others, include micro and macro encapsulation, shape stabilisation and porous inclusion (Sharma, et al., 2022).

Microencapsulation involves encasing PCMs in polymeric shells, creating microcapsules ranging from 1 to 300 micrometres (Liu, et al., 2017). These microcapsules, called MPCMs, have been tested for the use in building components like walls, roofs, and floors (Konuklu, et al., 2015). However, MPCMs have limitations, including lower stiffness and strength which are not practical for building applications. Furthermore, the risk of PCM leakage during mortar mixing, which can weaken the mortar, has been reported in different studies (Giro-Paloma,

et al., 2016), (Hunger, et al., 2009). Macroencapsulation is like microencapsulation but uses larger containers such as tubes or panels exceeding 1 cm in size (Liu, et al., 2017). These components can serve as building elements. However, like MPCMs, they also suffer from issues like leakage, as well as low heat transfer, and solidification at the container edges due to the large container sizes (Jawaid & Khan, 2018). This can prevent the encapsulated PCMs to undergo full heating and cooling cycles. The third technique utilises supporting materials like high-density polyethylene and styrene-butadiene-styrene to shape-stabilise PCMs (Jeon, et al., 2023). This process results in PCMs with a high apparent specific heat, shape stability during phase change, and no requirement for separate containers. However, this approach has a disadvantage: the shape-stabilised PCMs have lower thermal conductivity, which can limit their widespread use as the lower thermal conductivity can prevent the PCM gaining the right thermal energy for phase transition (Cui, et al., 2015). The fourth method is porous inclusion technique, which is considered the most cost-effective option as it does not involve the fabrication of PCMs using expensive containing materials. Porous inclusion involves infusing PCMs into materials with high porosity; materials such as expanded perlite, zeolites, expanded clay aggregates or biochar (Aguayo, et al., 2017). The resulting composite between PCMs and these materials can enhance thermal storage capacity in building materials. Research on PCMs-impregnated lightweight aggregates and their impact on both thermal and mechanical properties has been extensively explored (Haider, et al., 2022), (Sukontasukkul, et al., 2020). In this context, the porous inclusion technique emerges as a compelling avenue for further investigation. This method leverages the unique properties of porous materials, which can enhance thermal storage while potentially mitigating some of the challenges seen in other techniques. This paper presents an innovative approach to enhancing building materials by employing porous inclusion techniques to create PCM-biochar composites, specifically for integration into mortar and gypsum. Unlike conventional methods, this study utilises a cost-effective technique that leverages the high porosity of biochar to improve the compatibility of PCMs with building materials, resulting in composites with superior thermal storage capabilities compared to standard alternatives.

This research focuses on the integration of octadecane, a PCM with high latent heat capacity, and pinecone biochar, known for its environmental benefits, into building materials. This novel combination not only enhances the thermal performance of mortar and gypsum but also contributes to sustainability by improving energy efficiency in both new constructions and retrofitted buildings. The incorporation of PCM-biochar composites facilitates significant reductions in energy consumption and CO_2 emissions, addressing key challenges in energy efficiency and environmental impact. Biochar's role extends beyond being the carrier material for the PCM; it also imparts pozzolanic activity to the composites. This activity involves the reaction of biochar with calcium hydroxide, a by-product of cement hydration, forming additional cementitious compounds like calcium silicate hydrates (C-S-H) (Hewlett, et al., 1998) that enhance the strength and durability of mortar and concrete (Bernal, et al., 2017). Furthermore, the use of biochar allows for the sequestration of approximately 2.0 to 2.6 tonnes of CO_2 per tonne of biochar through carbonation (Azzi, et al., 2019), making it a highly sustainable material (Renforth, 2022). Finally, the use of biochar is considered sustainable and reduces waste, as biochar can be obtained as a by-product using biomass as fuel or by incineration of biomass waste such as organic waste, farming waste and salvage wood (Yuqing Sun, et al., 2021), (Shaheen, et al., 2019), (Liu, et al., 2021). This approach represents a

significant advancement in the field of building materials, offering the dual benefits of enhanced performance and a reduced carbon footprint.

Materials

Biochar

The biochar used in this research was produced through incineration of pinecone at a temperature of 600 °C and had particle size range of 0.01 – 8.0 mm. Biochar was chosen for its capacity to host PCM in its porous structure together with its suitability for utilisation as an aggregate in cementitious mix (Akinyemi & Adesina, 2020). The mean particle size of biochar was confirmed to be 2 mm using the "British Standard Aggregates for Concrete (BS EN 12,620)" (British Standard Institution, 2013). The biochar sample was sieved to remove any granules smaller than 1 mm, as these granules would reduce the workability of the cement mortar as they can fill the gap between the larger granules and reduce the internal friction (Harini, et al., 2012). In addition, the smaller size granules can be difficult to handle as they could pass through the mesh container used during impregnation. To remove any moisture from biochar, the granules were left to dry at 80 °C for a minimum of 3 days until constant mass. The biochar granules were found to be 71% porous with a water absorption capacity of 155 wt.%, calculated according to 'British Standard Tests for Mechanical and Physical Properties of Aggregates - Determination of Particle Density and Water Absorption (BS EN 1097-6)' (British Standard Institution, 2022) and a density of 267.7 $kg.m^{-3}$, calculated according to 'British Standard Tests for Mechanical and Physical Properties of Aggregates - Determination of Loose Bulk Density and Voids (BS EN 1097-3)' (British Standard Institution, 1998). The experimental BET surface area of the biochar samples was measured at 200 $m^2.g^{-1}$. The total pore area was 25.284 $m^2.g^{-1}$ at a pressure of 59,983.78 psia, while the median pore diameter was 15,763.81 nm, corresponding to a pore volume of 0.747 $mL.g^{-1}$ at 11.47 psia.

Pozzolanic activity measurement of biochar

The Chapelle test (NF P18-513) (Bézard, 2002) was used to measure the pozzolanic activity of biochar. In the Chapelle test, a sample of biochar (1 g) and calcium oxide powder (2 g) were added to 0.025 L of deionised water (the solvent); the mix was then stirred for 16 hrs at a temperature of 90 °C. The resultant slurry was then cooled before adding 0.25 L of 0.7 $mol{\cdot}dm^{-3}$ sucrose. After the addition of sucrose, the mix was stirred for 15 minutes and then the suspension was filtered. Finally, a few drops of 0.1% phenolphthalein were added to the filtrated solution, followed by titration with HCl (0.1 $mol{\cdot}dm^{-3}$). The pozzolanic activity was then determined using the titration results, as shown in *Equation 3* (Bézard, 2002)` below:

The reaction is as follows:

$$CaO + 2HCl \rightarrow CaCl_2 + H_2O \qquad \text{Equation (1)}$$

$$Ca(OH)_2 + 2\,HCl \rightarrow CaCl_2 + H_2O \qquad \text{Equation (2)}$$

$$\text{Ca (OH)}_2 \text{ fixed in mg } = 2\,\frac{(V_1 - V_2)74}{V_1 \quad 56} \times 1000 \qquad \text{Equation (3)}$$

Where:

- The volume of HCl solution required for blank samples without biochar is V_1.
- The volume of HCl solution required for samples with biochar is V_2.
- The values 74 and 56 refer to the molar masses of calcium hydroxide and calcium oxide, respectively, which are 74 g.mol^{-1} and 56 g.mol^{-1}.

The amount of calcium hydroxide formed during titration, measured in milligrams, indicates the pozzolanic activity.

Finally, powder X-ray diffraction (XRD) was used to determine the mineralogy of biochar, mortar, and PCM-biochar-mortar samples (Skevi, et al., 2022). This provides insights into their structural properties and mineral phases present within the samples of mortar and biochar after mixing and curing.

Phase change material & other materials used

Octadecane, a PCM with a melting point of 23 °C and latent heat of 227 J.g^{-1}, was selected for the experiment. A technical grade (purity of 95%) PCM was purchased from Sigma Aldrich. Other materials used were Portland limestone cement (CEM II/A-L 32.5R) purchased from Tarmac Blue Circle, UK; Gypsum purchased from British Gypsum, UK; deionised water; and standard silica sand purchased from Société Nouvelle Du Littoral, France.

Methodology

PCM impregnation of biochar

Two methods were tested to impregnate the biochar granules with octadecane. The first was an immersion method (Fig. 1), in which biochar granules are placed in molten octadecane (Ling & Poon, 2013). The second method was vacuum impregnation, in which a pressure differential is used to push octadecane inside the biochar pores (Fig. 2). Vacuum impregnation of octadecane is process inspired by the method of sealing leak paths that form during the aluminium casting process (Majumder, 2020).

For both methods, samples were produced in batches of 100 g of biochar, using a fine mesh basket filled with biochar and immersed into molten octadecane. Following impregnation, the biochar granules were surface dried on absorbent paper to remove any excess octadecane attached to the surface. Viscosity tests were conducted on the octadecane using a rheometer instrument called “Discovery Hybrid Rheometer”. The measurements were conducted between the temperatures range of 25 °C to 125 °C at a ramp of 3 °C. min^{-1} to evaluate how the temperature affects the absorption of octadecane into biochar when using the immersion and vacuum impregnation method (Johansson, et al., 2016).

Impregnation by immersion

Biochar granules were immersed in octadecane for 1 hr to allow the biochar to absorb molten octadecane into its pores. The molten octadecane was placed in a container, which was maintained in a water bath at a specific temperature of 70 °C, above its transition temperature of octadecane, so it would remain molten throughout the immersion process. After 1 hr the biochar granules were removed from the mesh basket. The PCM Percentage Absorption (PPA) was determined from the increase in mass of the biochar granules after immersion (See *Equation 4*). The percentage mass values were used to calculate the theoretical latent heat of PCM-biochar granules.

$$\text{PPA (\%)} = \frac{M_A - M_B}{V_D} \times \frac{1}{PCM_p} 100 \qquad \text{Equation (4)}$$

Where:

- M_A is the mass of PCM-biochar particles.
- M_B is the mass of the biochar.
- V_D is the dry volume of biochar.
- PCM_p is the density of the octadecane (Camp, 2017).

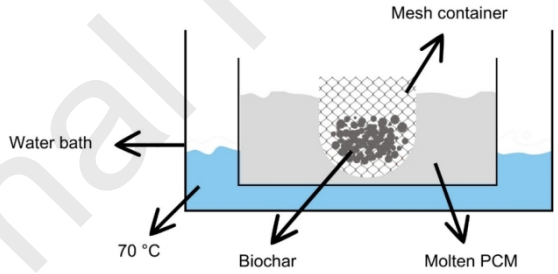

Fig. 1: Schematic of biochar impregnation by immersion method

Vacuum impregnation

In this method, a vacuum pump was used to remove air and moisture from the biochar pores, forcing the octadecane into these pores. In this method, biochar granules were placed in a mesh basket which was then placed in a desiccator filled with solid octadecane as shown in Fig. 2. Air and moisture were successfully extracted from the biochar pores by applying a pressure of 2 bar for 30 minutes, while keeping the temperature below the melting point of octadecane. After 30 minutes, the octadecane PCM was melted by raising the water bath temperature to 70 °C (See Fig. 2). This was done after the vacuum suction was turned off. The

biochar was then submerged into molten octadecane for 45 minutes. The impregnated biochar granules were removed and surfaced-dried.

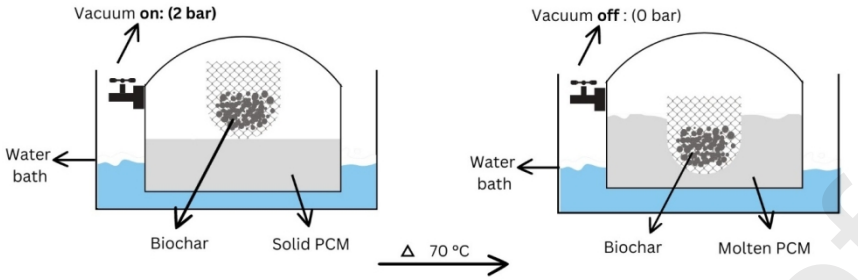

Fig. 2: Impregnation by vacuum impregnation schematic

PCM and PCM-biochar characterisation methods

Octadecane and PCM-biochar phase change temperatures and latent heat energy were analysed using Differential Scanning Calorimetry (DSC). DSC is useful for determining the thermodynamic properties such as phase change temperature and enthalpy. The tests were conducted at a ramping rate of 5 °C.min^{-1} over a temperature range of – 25 °C to 80 °C, under a flow of nitrogen gas (Kalnaes & Jelle, 2015). DSC analyses were conducted using an NETZSCH STA 449 F1 Jupiter thermal analyser.

An octadecane leakage test was conducted to evaluate any possible leakage of the PCM from the biochar. Once PCM-biochar granules were produced, leakage test was performed by placing the granules on filter paper for 3 hrs and raising the temperature gradually until leakage is observed or up to 80 °C. The high-temperature mass retention of PCM-biochar was assessed using thermogravimetric analysis (TGA). The analysis was performed at a heating rate of 10 °C. min^{-1}, up to a maximum temperature of 300 °C, under a continuous flow of nitrogen gas. While thermal cycling was not initially within the scope of this study, preliminary testing was conducted to ensure a comprehensive evaluation of the PCM-biochar composites. The stability of the PCM-biochar composite was assessed through an accelerated thermal cycling technique (Katish, et al., 2024), with samples subjected to 300 thermal cycles. The goal was to observe any changes in key thermal properties, specifically the phase change temperature and latent heat energy, to determine the material's long-term stability. The thermal stability of PCM-biochar granules was evaluated through thermal cycling of a 7 g PCM-biochar sample using DSC. The cycling conditions were set at a rate of 15 °C. min^{-1}. Each cycle included heating from 25 °C to 80 °C, cooling from 80 °C to -25 °C, and then reheating from -25 °C to 25 °C, all under nitrogen gas. Achieving 300 thermal cycles represents a significant milestone, as documented in my previous studies on PCMs' thermal stability and other relevant literature (Katish, et al., 2024).

To evaluate the interaction between biochar and the PCM, we employed four different techniques, each providing unique insights into the material properties and interactions. Scanning Electron Microscopy (SEM) was used to assess the microstructural details of the biochar-PCM composites, allowing us to observe the dispersion and bonding of PCM within the biochar matrix. Small-Angle X-ray Scattering (SAXS) investigated the phases available after combining PCM with biochar. Solid-State Proton Nuclear Magnetic Resonance (^{1}H NMR) studied the molecular dynamics and interactions at the atomic level, providing information on the mobility of hydrogen atoms and offering insights into the molecular interactions. Reflection Powder X-ray Diffraction (PXRD) identified the crystalline phases present in the composites, determining any changes in the crystalline structure of the PCM and any new phases formed as a result of their interaction. These techniques collectively provided a comprehensive understanding of the PCM-biochar interaction at molecular-level interactions.

Preparation and testing of mortar samples

Portland limestone cement (CEM II/A-L 32.5R), deionised water, standard silica sand, and PCM-biochar granules were used to manufacture a series of mortar samples, the proportions which are given in Table 1. The samples were prepared with a water-cement mass ratio of 1:2 and a cement-sand mass ratio of 1:3. The PCM-biochar granules were added as a replacement for the sand to in the total volume of mortar, expressed as the apparent volume of sand (v/v%).

All the mortar samples were manufactured following the procedures outlined in 'British Standard - Methods of Testing Cement Determination of Strength (BS EN 196-1)' (British Standards Institution, 2016). After mixing the mortar were poured into prism moulds for mechanical testing. At 23 °C and 40 % Relative Humidity the samples were cured for 24 hrs, then the samples were demoulded and left to cure in a water Bath at 2 °C for 28 days and 120 days.

Table 1: Mix proportions for mortar samples (percentage of sand replacement by volume).

Mix (Volume replacement)	**0%**	**10%**	**20%**	**30%**	**40%**	**50%**
Sand (g)	1350	1215	1080	945	810	675
PCM-biochar granules (g)	0	45	89	134	179	223

To measure the consistency of the fresh mortar; workability of the fresh mortars made with PCM-biochar granules was tested using the flow table method (British Standards Institution, 2016).

The compressive strengths and flexural test of mortars containing different percentages of PCM-biochar granules were determined in accordance with BS EN 196-1 using a Controls Automax 5 2000 kN compression machine; a 100 kN Dartec Servo hydraulic press and mortar samples after 28 and 120 curing days. Compressive strength was measured by placing the sample in a cube crusher with a contact area of 40 mm^2. Flexural strength was measured using a three-point flexural test and a displacement rate of 0.5 $mm.min^{-1}$. Both strength tests were done on a total of three replicas per mix sample.

Using a Hot Disk TPS 500 Thermal Analyser, the thermal conductivity and specific heat capacity of the samples were also tested. The instrument supplies a heating power to the sample tested for a measured period of time, with the temperature increase measured. The relationship between heat supplied and temperature increase of the sample tests allows the software to calculate the thermal conductivity and specific heat capacity (Ashraf, 2014).

Dry bulk density of hardened mortars was also determined according to 'British Standard for Determination of Dry Bulk Density of Hardened Mortar (BS EN 1015-10)' (British Standards Institution , 1999), using the compressive strength samples; the samples were left to dry at 50 °C until a constant mass was measured. The porosity, and water absorption measurements of the mortar samples were carried out on the samples recovered from the crushed materials after the compressive strength tests.

Preparation and testing of gypsum samples

PCM-biochar granules, gypsum plaster, and deionised water were used to produce a series of gypsum-PCM samples, with proportions given in Table 2. The samples were manufactured with a water plaster mass ratio of 3:5 and PCM-biochar granules replacement between 10% to 50% Vol. of gypsum, as shown in Table 2. All gypsum samples were manufactured according to 'British Standard Gypsum Binders and Gypsum Plasters - Definitions and Requirements (BS EN 13279-1)' (British Standards Institution , 2009), with the PCM-biochar granules added simultaneously with the gypsum.

After mixing the fresh gypsum was cast into sets of prisms for mechanical and thermal conductivity testing. The samples were left to cure at 20 °C and RH of 40% in a controlled environment and tested after 28 days. While gypsum typically has a shorter setting time, the plaster was allowed to cure for this duration to facilitate a meaningful comparison with the cement mortar sample.

Table 2: Mix proportions for gypsum samples (percentage of each component of the mix).

Replacement percentage (%)	**0%**	**10%**	**20%**	**30%**	**40%**	**50%**
Gypsum (g)	1200	1080	960	840	720	600

Water (g)	720	648	576	504	432	360
PCM-biochar granules (g)	0	150	300	450	600	750

The compressive strength and flexural strength of gypsum samples were tested using the same instrument and procedures applied to the mortar samples, following BS EN 196-1, after 28 days of curing. The thermal conductivity and density were measured using the same methods as used for the mortar samples.

Results and discussion

PCM-biochar impregnation tests

Fig. 3 shows the octadecane percentage absorption as wt.% vs the ratio of PCM:biochar for the two impregnations methods used to load the biochar granules, immersion, and vacuum impregnation. PCM-biochar. The ratio PCM:biochar represents the initial quantities of each substance utilised at the onset of each experiment. The quantity of PCM introduced in each trial increases proportionally to the mass of the biochar. The findings of these trials indicate that the differences in absorption between the two impregnation methods were generally significant, with the absorption of octadecane being always larger for the vacuum impregnation method. The most noticeable distinction occurred at a PCM-biochar ratio of 2.5:1.0, where vacuum impregnation resulted in a 34.48 % higher loading compared to immersion. When the PCM-biochar ratio was increased further, the observed increase in PCM loading into biochar was negligible. Hence 2.5:1.0 was selected as the optimum ratio for impregnating octadecane into biochar. Other parameters such as vacuum impregnation pressure (2 bar) and water bath temperature (70 °C) were selected as the optimum impregnation conditions as no significant impregnation was observed when pressure and temperature increased. The viscosity of octadecane was measured using a rheometer at 25 °C, 40 °C, 70 °C, 100 °C, and 125 °C and was found to be 3.80 mPa.s, 3.05 mPa.s, 2.54 mPa.s, 1.39 mPa.s, 1.14 mPa.s, and 0.87 mPa.s, respectively. Hence, 70 °C was determined as the temperature at which impregnation will be carried out. This is because at 70 °C octadecane is less viscous, above 70 °C, the impact of temperature on viscosity becomes trivial for the amount of heat input. Although it is possible to carry out the impregnation at higher temperature, this would increase the embodied energy of PCM-biochar manufactured granules. Based on these findings, it was determined that the ideal impregnation ratio was determined to fall within the range of 2.5:1.0 to 3.0:1.0. The highest volume absorption achieved through vacuum impregnation reached 62.21 %.

The methods employed for impregnating PCM into biochar in this study demonstrated favourable results in achieving a considerable impregnation level compared to alternative methods, see Table 3. Although our method did not reach the highest impregnation level, the significant latent heat energy of the PCM used (227 J. g^{-1}) enabled the development of a composite with a notable latent heat energy of 116.7 J. g^{-1}. For comparison, Hussein et al. (2015) achieved 36.42% impregnation and a latent heat energy of 107.2 J. g^{-1} using octadecane and peat soil (Hussein, et al., 2015), while Jeon et al. (2019) reported 49.72% impregnation and 92.13 J. g^{-1} latent heat with palm wax in rice husk (Jeon, et al., 2019). Atinafu et al. (2020) reached 38.13% impregnation and 91.5 J. g^{-1} latent heat with octadecane and PEFC (Atinafu, et al., 2020). Similarly, Hussein et al. (2020) obtained 44.66% impregnation and 87.42 J. g^{-1} latent heat with octadecane and palm kernel shell (Hussein, et al., 2020).

Further, Jeon et al. (2019) achieved 65.09% impregnation and 74.6 J. g^{-1} latent heat with coconut oil and pine sawdust biochar (Jeon, et al., 2019). Wadee et al. (2022) reported varying latent heat values for different PCMs, with RT18HC reaching 70.7 J. g^{-1}, RT22HC at 54.7 J. g^{-1}, and RT25HC at 50.1 J. g^{-1} (Wadee, et al., 2022). Sani et al. (2021) and G et al. (2020) achieved lower latent heat values of 39 J. g^{-1} and 56.2 J. g^{-1}, respectively, using fly-ash aggregates and sewage sludge biochar, (Sani, et al., 2021) (G, et al., 2020).

On the other hand, research conducted by Pisello et al. on vacuum impregnation of PCM into biochar using various types of commercial PCMs has yielded higher latent heat values for PCMs operating at temperatures of 27 °C and 31 °C (Fabiani, et al., 2023). It is noteworthy that although the latent heat energy of these PCMs is less than that of octadecane (185 $J.g^{-1}$ and 165 $J.g^{-1}$ for RT27 and RT31, respectively), the experimental latent heat energy value for the PCM-biochar composite with these PCMs surpasses the theoretical latent heat energy expected for composites. Specifically, the theoretically expected latent heat energy was found to be 100.60 J. g^{-1} and 101.73 J. g^{-1} compared to the experimental 130.92 J. g^{-1} and 117.96 J. g^{-1}. The theoretical latent heat energy is the maximum energy that could be achieved which is equal to experimental latent heat energy at 100% efficiency. The reason behind this discrepancy is not entirely clear. Further investigation is required to explain the precise mechanisms underlying the observed differences and to optimise the impregnation process for achieving even higher latent heat values in PCM-biochar composites.

Table 3: Comparison with Other PCM Impregnation into Porous Materials Studies for Built Environment Applications.

PCM	**Carrier Material**	**Impregnation Method**	**Impregnation value (wt.%)**	**Latent Heat Energy (J. g^{-1})**	**Reference**
Octadecane	Biochar	Vacuum Impregnation	62.21 (±0.29)	116 (±10%)	This study
Octadecane	Peat soil	Immersion	36.42	107.20	(Hussein, et al., 2015)
Palm wax	Rice husk	Vacuum Impregnation	49.72	92.13	(Jeon, et al., 2019)
Octadecane	Polyethylene-co-vinyl acetate (PEFC)	Vacuum Impregnation	38.13	91.50	(Atinafu, et al., 2020)

Octadecane	Palm kernel shell	Immersion	44.66	87.42	(Hussein, et al., 2020)
Coconut oil	Pine saw dust biochar	Vacuum Impregnation	65.09	74.60	(Jeon, et al., 2019)
RT18HC	Lightweight aggregate	Vacuum Impregnation	60.87	70.7	(Wadee, et al., 2022)
RT22HC			61.49	54.7	
RT25HC			63.01	50.10	
PCM1	Fly–ash aggregates	Vacuum Impregnation	18.56	39	(Sani, et al., 2021)
1-dodecanol	Sewage sledge biochar	Vacuum Impregnation	25.77	56.2	(G, et al., 2020)
RT31	Biochar	Vacuum Impregnation	60.97	130.92	(Fabiani, et al., 2023)
	Lignin		12.81	27.84	
RT27	Biochar		54.99	117.96	
	Lignin		24.99	32.52	
RT21	Biochar		67.37	74.64	
	Lignin		22.33	22.80	

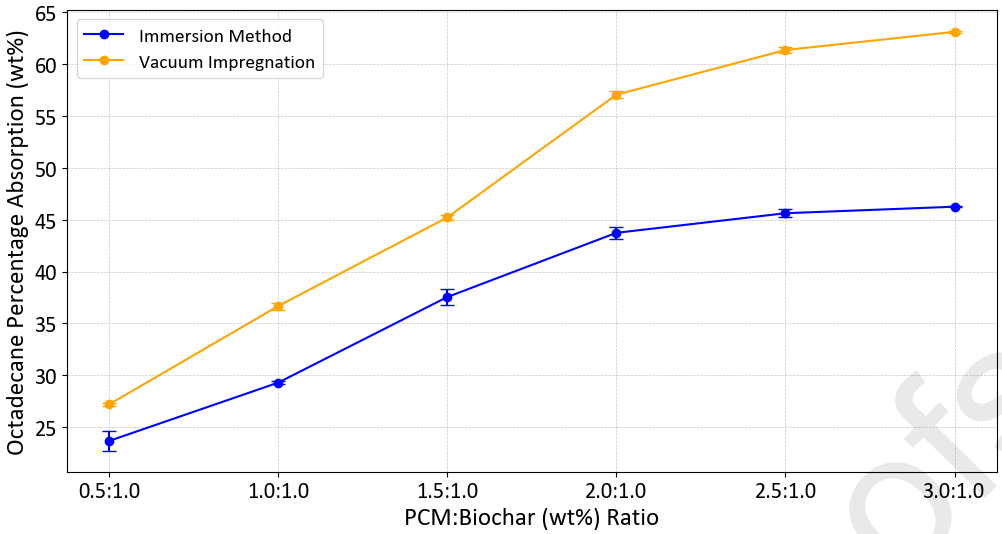

Fig. 3: Octadecane percentage absorption as wt% vs the ratio of PCM:biochar for the two impregnations methods used to load the biochar granules.

Differential scanning calorimetry (DSC)

To accurately evaluate the thermal properties of the produced PCM-biochar granules, DSC was utilised to determine the enthalpy before and after absorption. Fig. 4 shows the DSC measurements for the pure PCMs, biochar and the PCM-biochar granules. The PCM exhibited a wide exothermic peak indicative of energy release during the solidification process and a broad endothermic peak representing energy absorption during the melting process. These peaks shared similar shapes and areas but displayed a noticeable temperature offset. This temperature offset indicatives that the PCM undergoes melting during heating and solidification during cooling. Utilising the curve, the onset phase change temperature and the corresponding enthalpy can be determined, which represents the amount of energy necessary for the transition. The integration of the area between the heat flow curve and the baseline facilitated this calculation. A comparison between the pure PCM, and PCM-biochar particles revealed a reduction in enthalpy for both melting and freezing processes in the latter. PCM-biochar has a latent heat energy of 116.7 (±10%) J. g^{-1}. This value can be compared with the theoretical latent heat energy of the PCM using *Equation 5* below:

$$L_T = L_{PCM} \times W_{PCM}\,\% \qquad \text{Equation (5)}$$

Where the latent heat energy of PCM is (L_{PCM}), and the percentage of vacuum impregnation is (W_{PCM} %).

The theoretical value of the PCM-biochar granules L_T is 141.22 J.g^{-1} which is 17.36% greater than the experimental value (116.7 (±10%) J.g^{-1}). This difference can be attributed to the complex and irregular pore structure of biochar having a negative impact on the heat transfer efficiency of the PCM within its pores. The DSC instrument has an error margin of ± 10%. Hence, the actual difference between theoretical and experimental value can vary. Furthermore, several studies have reported a lower experimental latent heat energy when

compared to a theoretical latent heat energy measurement (Sarı, et al., 2018) (Karaipekli & Sarı, 2009).

Finally, PCMs require a carrier to be effectively integrated into building materials, as methods like microencapsulation or direct incorporation can result in more complex issues. Impregnating PCM into biochar, despite leading to a 42.48% reduction in latent heat energy, primarily due to the partial volumetric displacement of PCM by biochar, it remains a necessary approach for incorporating PCM into construction applications. This composite material remains viable for thermal energy storage, as the biochar enhances thermal management by improving thermal conductivity and reducing the risk of PCM leakage, which can otherwise compromise material performance. Additionally, the integration of biochar provides structural reinforcement and contributes to carbon sequestration, making the PCM-biochar composite not only a practical solution for energy-efficient buildings but also a sustainable material choice.

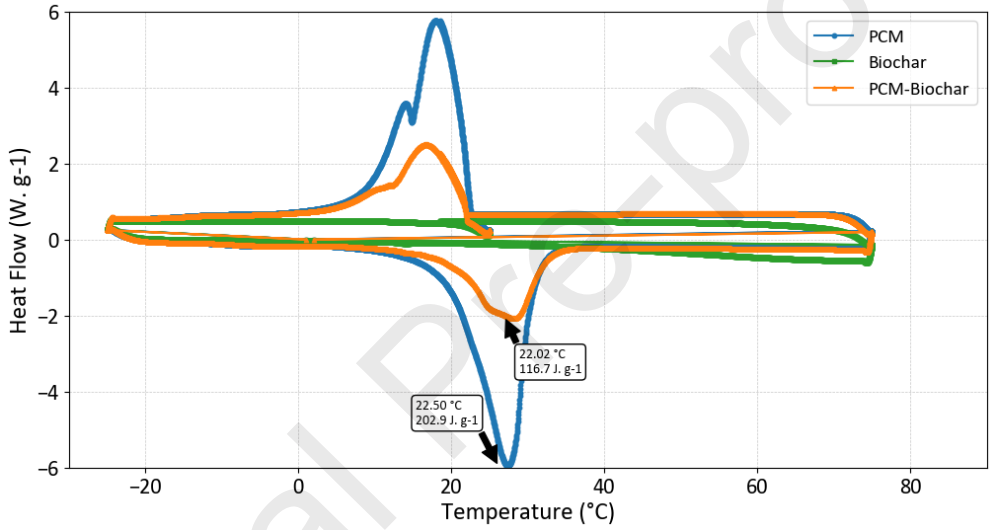

Fig. 4: DSC curve of the PCM (Octadecane), biochar, and PCM-biochar (Exo Up)

Thermogravimetric analysis (TGA)

Fig. 5 presents the TGA results for PCM, PCM-biochar, and biochar, providing insights into the thermal stability of PCM when combined with biochar. Understanding whether the incorporation of biochar impacts the stability of PCM at elevated temperatures is essential, particularly because PCMs must not undergo sublimation (a phase transition directly from solid to gas, bypassing the liquid state) or present any safety hazards. These factors are crucial for their effective use in building environments and other industries.

At the lower temperature of 30 °C, all samples PCM, PCM-biochar, and biochar exhibited no mass loss, indicating their stability and appropriateness for applications in such conditions. However, as the temperature increased beyond 150 °C, PCM began to gradually lose mass, ranging between 15 % and 20 %. This behaviour is typical for octadecane, attributed to thermal degradation and volatilisation. However, even at 170 °C, a significant portion of the PCM's initial mass remained intact. Yet, between 250 °C and 300 °C, the mass retention

sharply declined, leading to nearly complete mass loss by 300 °C. In contrast, PCM-biochar displayed lower thermal stability, with higher mass loss occurring after 170 °C approximately 19 %. This higher mass loss likely because biochar may contain volatile organic compounds, and residual moisture, that decompose or evaporate at lower temperatures than octadecane. This may have led to additional weight loss in the mixture. Additionally, after 200 °C PCM-biochar did not experience a complete mass loss of the PCM; which makes up approximately 62 % of the initial samples mass and the mass loss plateaued at 35 %. This may be due some of PCM being retained in the biochar's pores in the form of soot and char; (at elevated temperatures, the PCM octadecane undergoes thermal cracking, breaking down long hydrocarbon chains. As the temperature rises, carbonaceous residues, such as soot and char, start to form) (Faden, et al., 2019). The biochar itself showed minimal mass loss at 300 °C, as most of the easily volatilised organic compounds and moisture had already been released at around 50 °C to 100 °C, while the more stable carbonaceous structures had not yet significantly decomposed. This stabilisation at 300 °C marks a transition point, beyond which higher temperatures would be needed to break down the more resilient components of biochar.

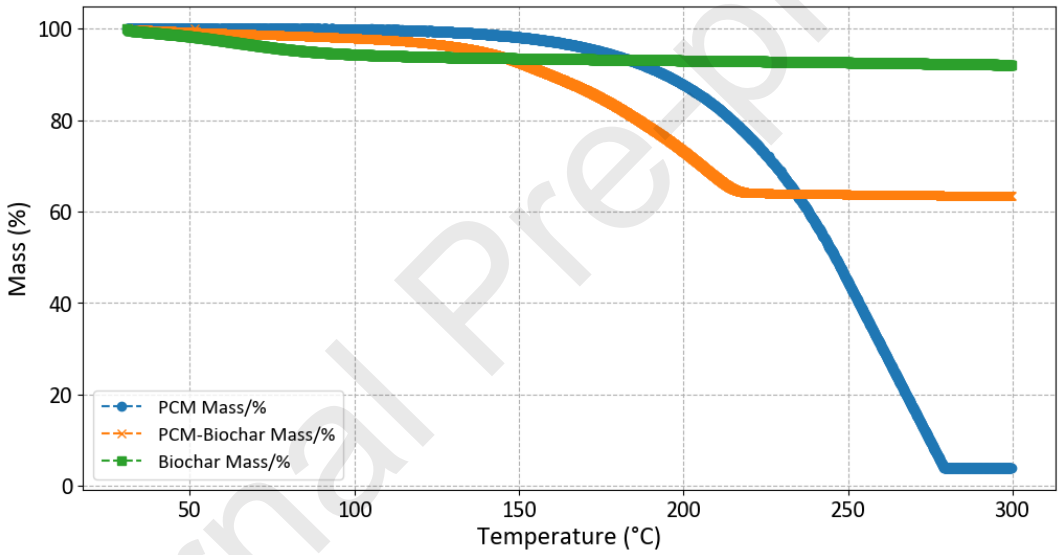

Fig. 5: Thermal stability measurements of PCM, PCM-biochar and biochar samples

Thermal stability of PCM-biochar granules under continual cycling.

The results shown in Fig. 6 demonstrated that the PCM-biochar composite maintained stability throughout the 300 thermal cycles, showing only minimal variation in thermal properties. The phase change temperature remained consistent within the machine's error rate of ±1°C, indicating that the material's melting and solidification points were not significantly affected by repeated cycling. Similarly, the latent heat energy of the composite showed only slight fluctuations within the acceptable machine error margin of ±10%, confirming the retention of the composite's energy storage capacity. For example, the phase change temperature and latent heat energy of the composite after 1 thermal cycle and 300 thermal cycles were 22.22 °C and 114.31 J. g^{-1} versus 21.09 °C and 113.67 J. g^{-1}, respectively.

One notable observation from the accelerated thermal cycling was the reduced subcooling effect at higher heating rates. Specifically, subcooling was less pronounced when using a heating rate of 15 °C.min^{-1} compared to 5 °C.min^{-1}, as illustrated in Fig. 6.

This stability is a significant indicator that the integration of PCM into the biochar porous does not adversely impact the thermal performance of the material over multiple heating and cooling cycles. Instead, it suggests that the composite can reliably undergo repeated thermal stresses without significant degradation in its thermal storage capabilities.

These findings align with the intended use of PCM-biochar composites in built environment applications where consistent thermal regulation over prolonged periods is required.

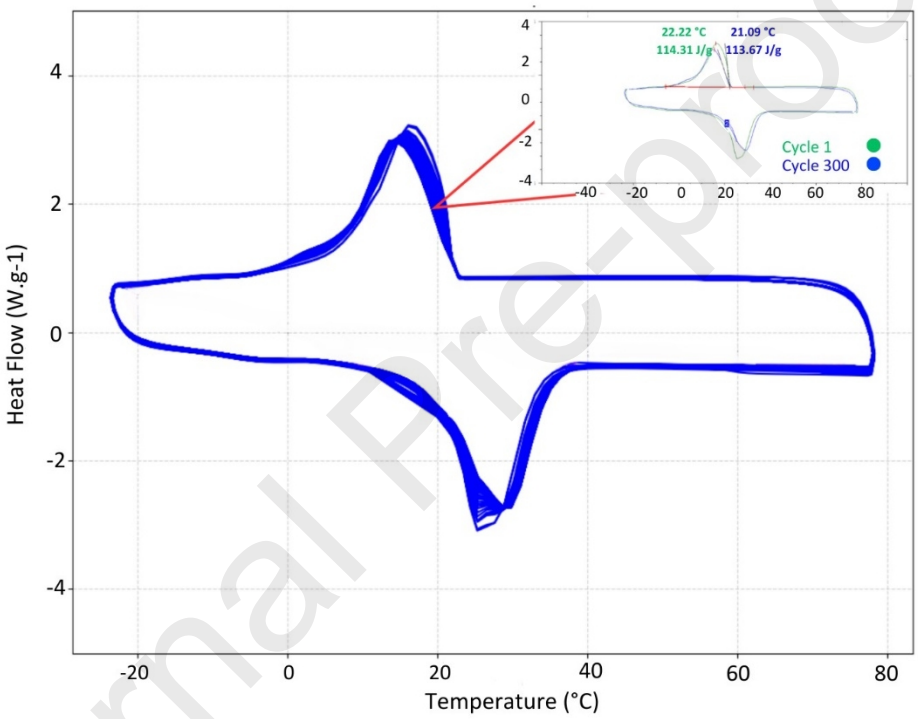

Fig. 6: Thermal cycling of PCM-biochar sample – 300 thermal cycles

PCM-biochar leakage test and interaction analysis

Fig. 7 presents a SEM scan of a partially fractured biochar and PCM-biochar sample. The scan illustrates the presence of PCMs within the biochar pores post-impregnation and drying. Fig. 8, displays the results of the PCM-biochar leakage test, demonstrating that the biochar effectively retains the PCM within its pores, while intensive leakage observed at higher temperature (See Fig. 8- F). Initially, the retention of PCM in biochar is thought to be due to the formation of a co-crystal (S. Schaefer a, et al., 2020). However, when subjecting a PCM-biochar sample to SAXS analysis (Fig. 9), no evident new phases emerged from this interaction. Instead, the results revealed a reduction in peak intensity of 47.2% for PCM-

biochar compared to PCM samples., This is in line with the DSC results discussed in section 3.2.1.

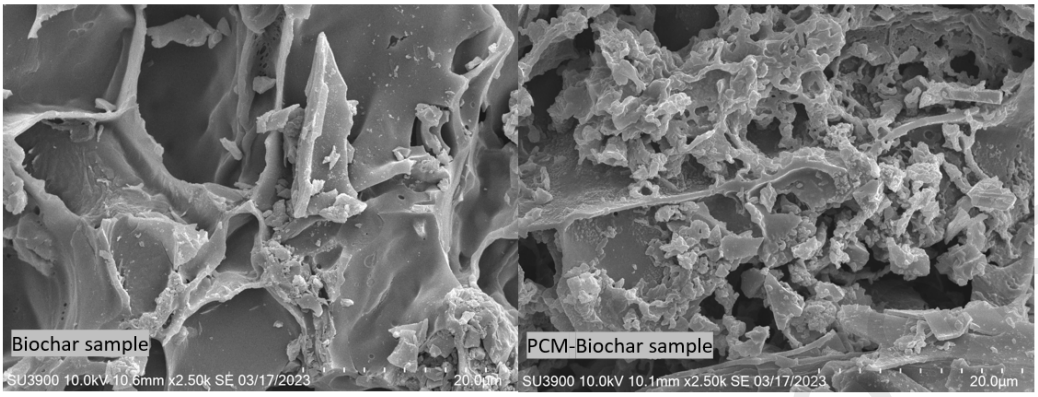

Fig. 7: SEM scan of biochar sample (Left) and PCM-biochar (Right)

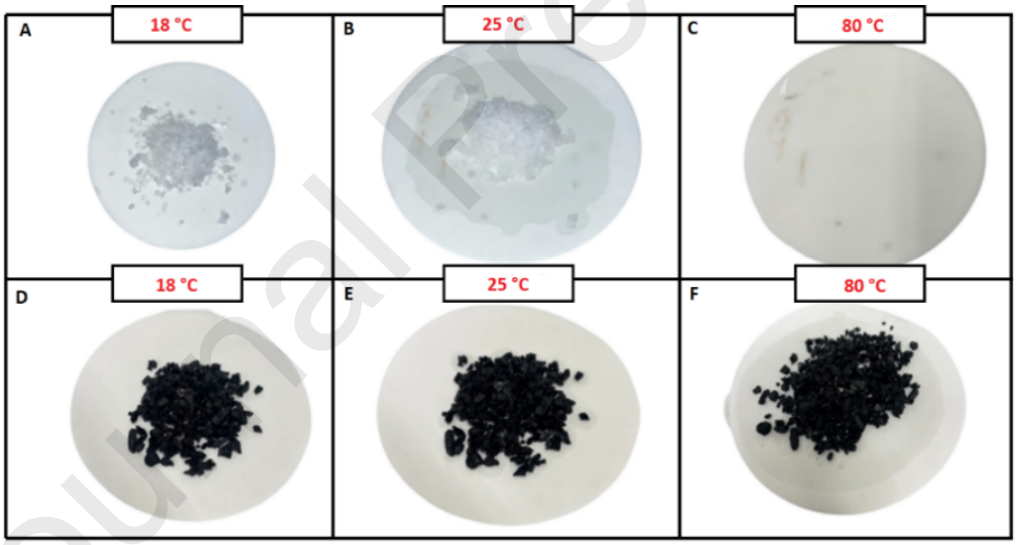

Fig. 8: Leakage test of PCM-biochar when increasing temperature from 18 °C to 80 °C - a comparison between PCM (top) and PCM-biochar (bottom)

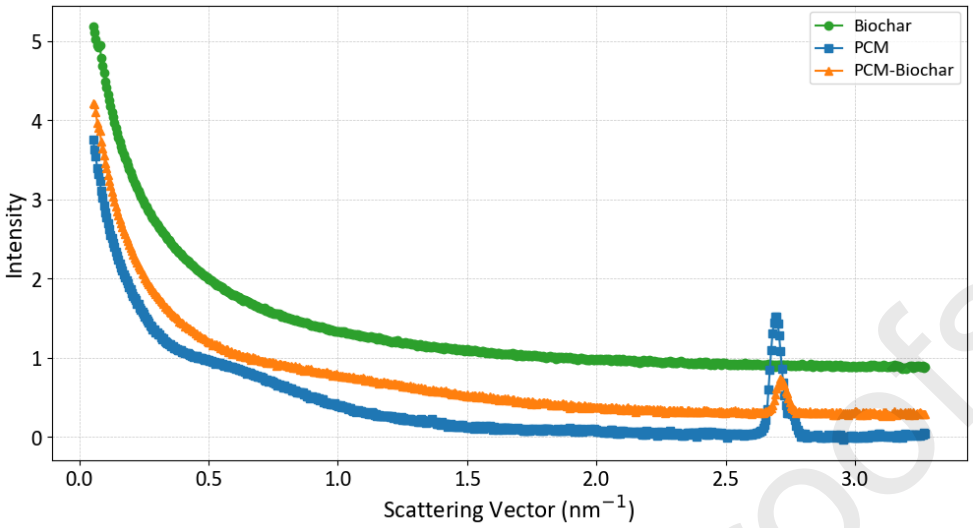

Fig. 9: SAXS scan of PCM, PCM-biochar and biochar showing phase changes available in the PCM, PCM-biochar, and biochar.

Finally, XRD pattern and Solid-Solid ^{1}H NMR were used to further study the interaction between PCM and biochar. This interaction was identified by observing noticeable changes in the positions and intensities of peaks in the XRD patterns or a shift in the ^{1}H NMR environment (Hadjipanayis, et al., 1992). XRD results in Fig. 10, show the interaction between PCM and biochar. Upon the combination of PCM with biochar, certain peaks in the XRD pattern undergo noticeable modifications. Specifically, PCM peaks at 35.5° and those within the range of 18° to 24° exhibit a significant reduction in intensity, nearly by 80%. On the other hand, biochar demonstrates changes in its peaks as well, with a peak at 27.5° disappearing entirely and another peak at 29.5° experiencing a reduction in intensity by approximately 70 %. These changes in peak intensities suggest an interaction between PCM and biochar. (Epp, 2016). Solid-State ^{1}H NMR of PCM, PCM-biochar and biochar also support an interaction between PCM and biochar, this is concluded when a ^{1}H NMR of PCM-biochar was taken new proton environments appeared at -25 ppm and 35 ppm (See Fig. 11 to Fig. 13). The interaction could be due to hydrogen atoms on octadecane interacting with the lone pairs of electrons on the oxygen atoms in biochar, through a type of bonding called dipole-dipole force (Weller, 2014). This type of bonding is weaker than ionic and covalent type of bonding and can be easily broken by increasing the temperature. This results in increasing the vibrational energies of the molecules within the composite. Hence, the retention of biochar to PCM is broken at elevated temperature as seen in Fig. 8 above. Therefore, meeting these specific conditions is crucial for extracting the PCM from the biochar pores.

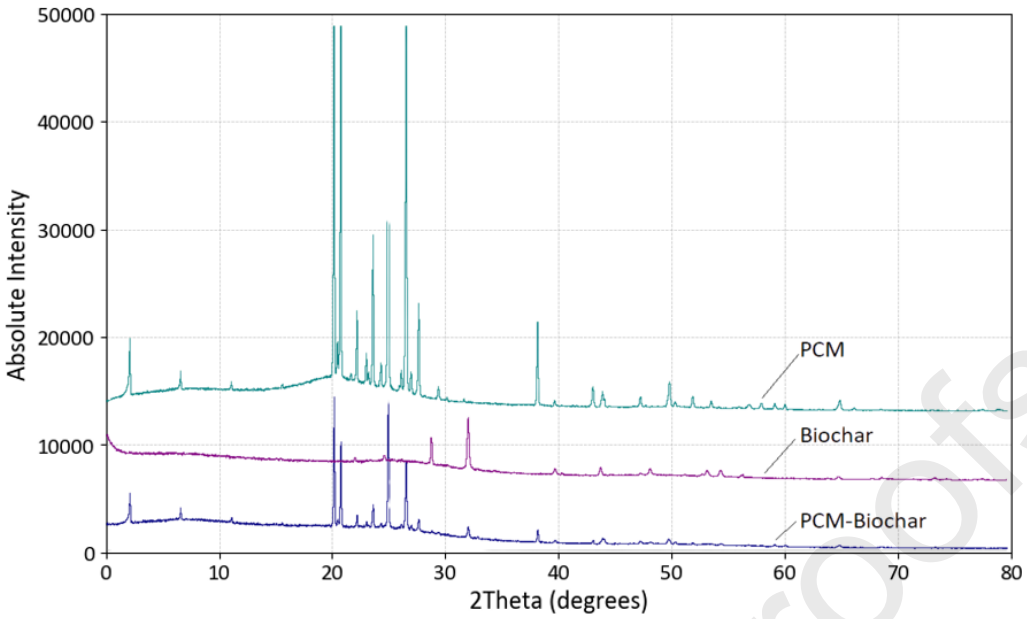

Fig. 10: PXRD scans of PCM, biochar and PCM-biochar samples

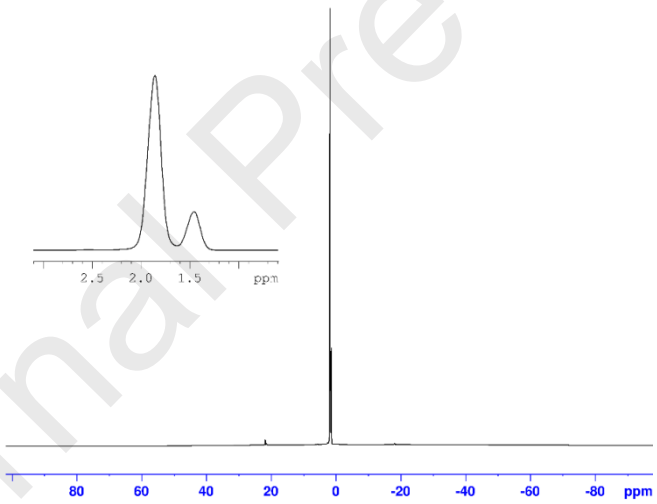

Fig. 11: Solid-State ^{1}H NMR of octadecane

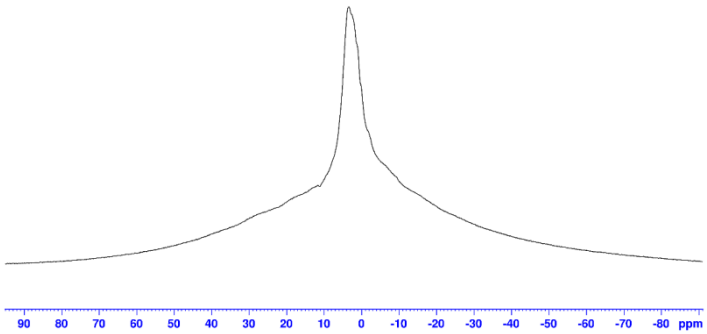

Fig. 12: Solid-State ^{1}H NMR of biochar

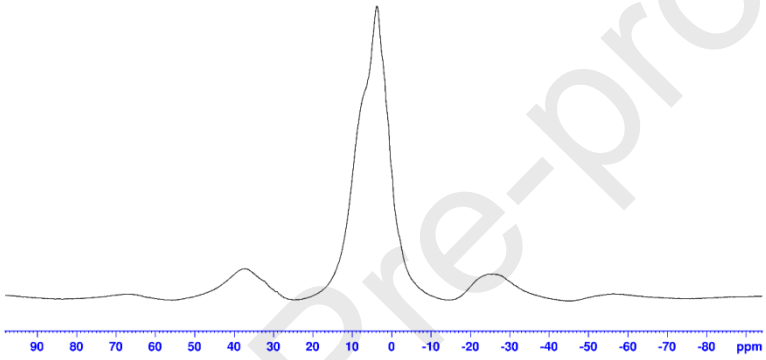

Fig. 13: Solid-State ^{1}H NMR of PCM-biochar

Pozzolanic activity measurement of biochar

The pozzolanic activity of biochar was tested using the Chapelle Test on three different biochar samples with varying mean particle sizes (See Table 4). The results shown in Table 4 indicate that the biochar sample used in this work is not pozzolanically active, as its pozzolanic activity index falls below 1000 mg. g^{-1}. The low pozzolanic activity of biochar could be resulted from the fact biochar lacks the necessary reactive components, such as adequate amounts of amorphous silica and alumina, to exhibit pozzolanic activity (Donatello, et al., 2010). Or it could be because these alkaline minerals are locked and need to be activated. The mineral availability in biochar could be unlocked using pretreatment processes such as mechanochemical activation, thermal activation or simply ball milling (S. Donatello & Cheeseman, 2010). These methods could improve the pozzolanic activity of biochar by releasing alkaline minerals trapped in it as well as increase the surface area of biochar granules (Santos & Cordeiro, 2021), thereby enhancing their adhesion to cement and improve the porosity of the overall mix. For instance, materials such as ground diatomite (Santos & Cordeiro, 2021); coal gangue calcined at 800 °C (Hao, et al., 2022); vacuum glass microspheres (Martín, et al., 2021); and modified clay (Leussa, et al., 2020) have shown a higher pozzolanic activity index than biochar; 1178 mg. g^{-1}, 1039 mg. g^{-1}, 1365 mg. g^{-1}, and 1121 mg. g^{-1},

respectively. The higher pozzolanic activity for the materials mentioned above was attributed to the pretreatments processes which these materials have gone through.

Table 4: Pozzolanic activity of three different samples of biochar

Biochar Samples	**Bet surface area ($m^2.g^{-1}$)**	**D50 (mm)**	**Pozzolanic activity (mg. g^{-1})**
Sample 1	56.97	0.695	262.062 (±1.12)
Sample 2	25.33	3.195	110.02 (±2.03)
Sample 3	0.84	7.32	7.64 (±1.06)

Furthermore, Fig. 14 shows the mineralogical composition of biochar, mortar, and PCM-Biochar-mortar composite (after 120 days). The findings reveal notable differences in mineral content among the samples. The biochar sample exhibits a relatively low fraction of calcites at 26.86° and alites at 28.11°; complementing the findings from Chapelle Test which indicated a low pozzolanic activity. Conversely, the mortar sample showcases a more diverse range of minerals, including portlandite at 18.10°, gypsum at 20.72°, calcite 28.11° and at 29.45°, alites 28.11°, dolomite at 34.15°, free lime at 36.70°, and periclase at 42.93°. In CEM II mortar, minerals like portlandite aid early strength, gypsum controls setting time, calcite and alite drive hydration forming calcium silicate hydrate gel for strength, dolomite affects workability and durability, while free lime and periclase react with water, aiding hardening (Sedaghat, et al., 2014). These minerals shape the mechanical and chemical properties of CEM II mortar, making it versatile for construction (Roussel, 2011). Interestingly, the incorporation of biochar into the PCM-Biochar-mortar mix, referred to as cement-biochar in Fig. 14, did not lead to the formation of new cementitious bonds. This suggests that biochar did not significantly contribute to the overall development of the mortar strength. One possible explanation for this observation has been already mentioned and it is that the alkaline minerals in biochar need to be released using pretreatment processes.

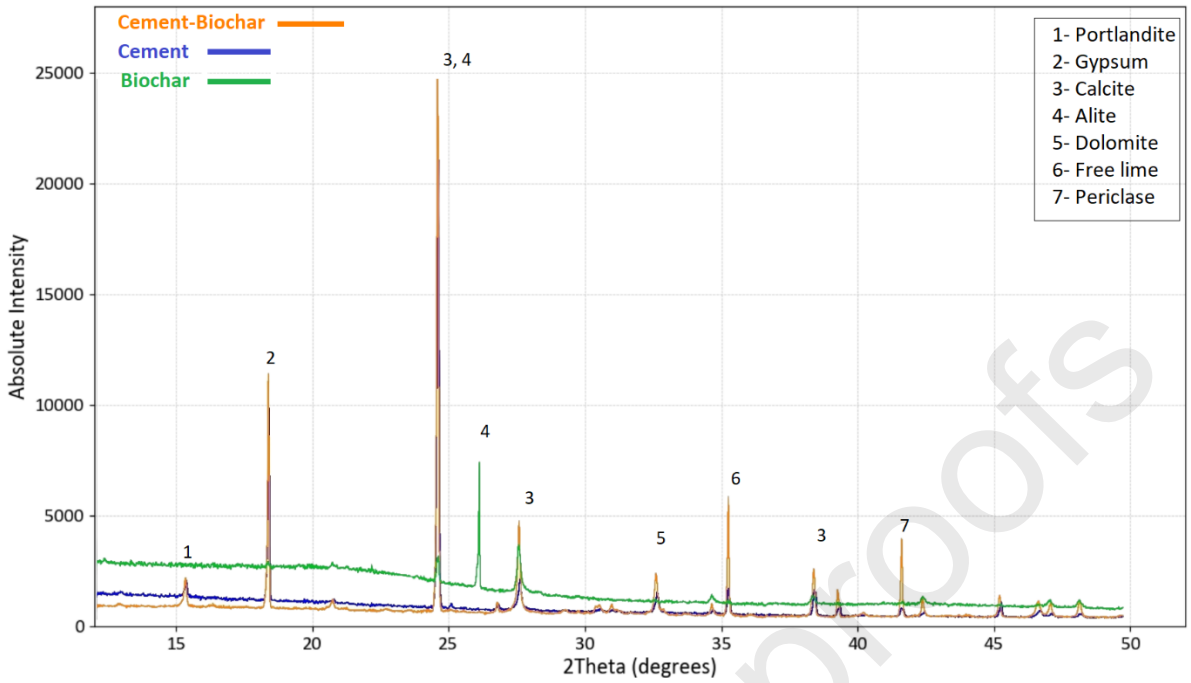

Fig. 14: XRD spectra of biochar, control mortar, PCM-biochar mortar. 1: Portlandite, 2: Gypsum, 3: Calcite, 4: Alite, 5: Dolomite, 6: Free Lime, 7: Periclase

Cement mortar workability test

The test results for the consistency of the control cement mortar (containing no PCM-biochar particles) and the cement mortars containing 10% to 50% PCM-biochar particles are shown in Fig. 15. The water-cement ratio was maintained at 1:2 to evaluate the impact of PCM-biochar replacement to sand on cement mixtures workability. The results indicate that increasing the percentage of PCM-biochar particles led to a consistent decrease in workability of the cement. This is caused by the porous nature of the biochar particles. Spherical sand grains necessitate a lesser quantity of water to attain the desired mixing consistency, whereas both larger angular and porous materials demand a greater amount of water to achieve equivalent workability (Haddad, et al., 2020). Uthaichotirat et. al, have also suggested that the workability of mortar is highly influenced by the shape and size of the PCM granules (Uthaichotirat, et al., 2020). In this study, the mortars were still considered workable for the highest replacement rate of 50

% PCM-biochar. It is important to maintain a workable mix as reduced workability is associated with diminished strength and durability.

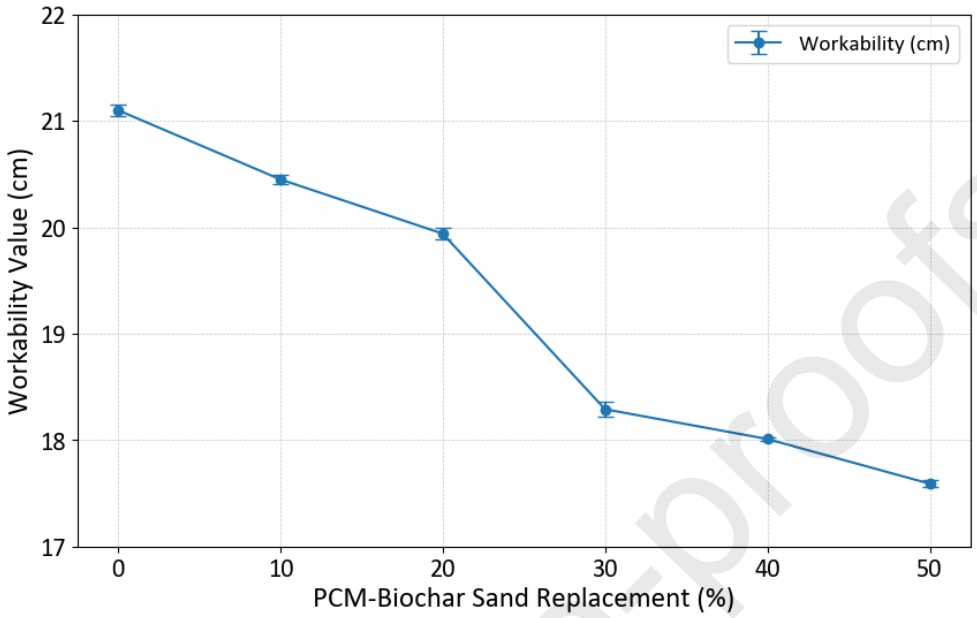

Fig. 15: Workability of fresh mortar, tested using flow table.

Cement mortar calorimetry

A number of studies have suggested that PCMs may potentially escape from host granules and disrupt the cement hydration process (Mehta, 2006) (Qi, et al., 2021). Cement hydration proceeds through five primary stages: (1) initial reaction, commencing promptly after water addition; (2) induction, a period of inactivity ensuring workability; (3) acceleration, an intensified reaction determining the rate of cement hardening; (4) deceleration, marked by a decline in hydration product formation affecting early strength development; and (5) a gradual and continuous reaction phase, characterised by steady hydration product formation impacting later strength gain (Kosmatka, et al., 2002) (Scrivener, et al., 2015). Isothermal calorimetry was employed on PCM-biochar particles mix with cement to evaluate the potential influence of PCM-biochar addition on cement hydration reactions.

As depicted in Fig. 16, two peaks are evident within the initial 12 hrs of hydration for each mix, with the first occurring at 0 hrs and the second at approximately 8 hrs for both the control and PCM-biochar loaded mortar. These peaks correspond to the initial reaction and induction stages of cement hydration. The first peak signifies the immediate reaction upon mixing cement with water, followed by an induction period and an acceleration phase at 1.5 hrs of hydration. Samples containing PCM-biochar exhibited a thermal power below 0 mW. g^{-1} during the induction period, likely due to temperature differences between the sample and the calorimeter. Heat absorption from the calorimeter to the specimen, with the calorimeter

temperature set at 30 °C, allowed the PCM to undergo a phase change, simulating a worst-case scenario to analyse the effects of PCM leakage.

Control results demonstrated typical behaviour for (CEM II/A-L) mortar, with maximum heat production around 8 hrs attributed to the formation of ettringite (Dehdezi, et al., 2013). Although Fig. 16 below shows that the hydration power is generally higher for the mix containing PCM-biochar, both mixes follow the same hydration pattern. The higher power could be a result of the reduced water cement ratio in the sample containing PCM-biochar, as the biochar could have absorbed some of the water resulting in a higher power measurement. Having said that, no noticeable delay in hydration is observed for the mix containing PCM-biochar particles over a 72 hrs period, suggesting that the addition of PCM-biochar particles does not affect hydration time, as illustrated in Fig. 16.

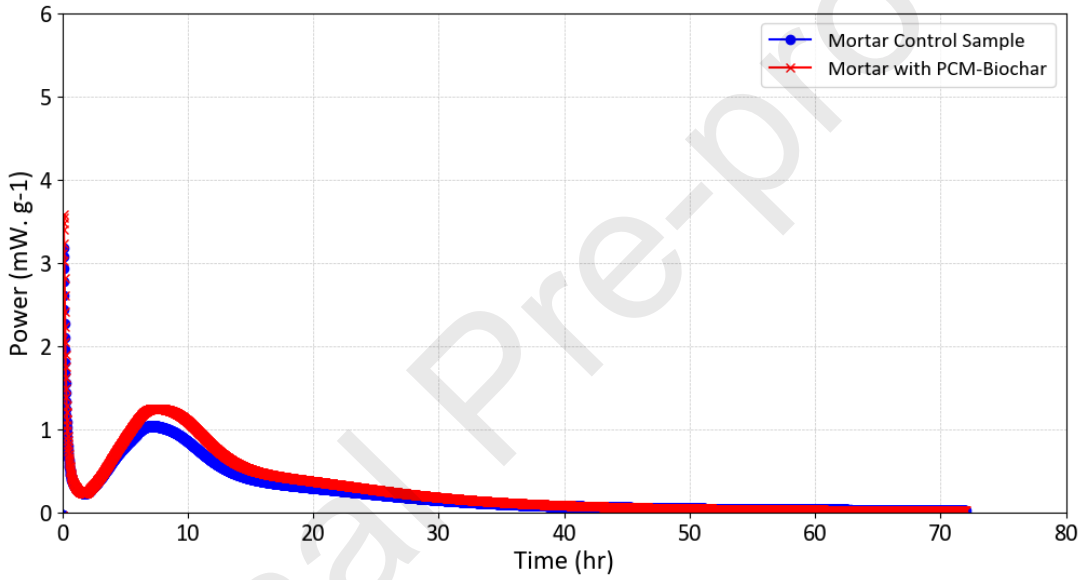

Fig. 16: Isothermal calorimetry is employed to observe the thermal power released during the hydration reaction of CEM II over a 72 hrs duration.

Cement mortar compressive strength

The results of compressive strength after 28 and 120 days of curing time are presented in Fig. 17, which shows the impact of PCM-biochar particle addition on the compressive strength of the cement mortar mixture. The observed trends provide valuable insights into the material's performance and potential implications for practical applications. The addition of PCM-biochar particles led to a noticeable reduction in compressive strength after 28 days of curing. As shown in Fig. 17, the mortar compressive strength declined as the percentage of sand replacement increased; for instance, for a PCM-biochar sand replacement of 10 % and 20 % resulted in a reduction in compressive strength of approximately 11.85 % and 18.29 %, respectively. This reduction in strength is attributed to the porous nature of biochar, which when incorporated into the mix, introduces voids and weak points in the mortar structure.

Additionally, the decreased workability of the mixture may contribute to a decrease in overall strength compared to traditional mortar formulation made using BS EN 196 (British Standards Institution, 2016). These findings align with previous studies reported by K.S. Elango et al. and (Elango, et al., 2021), who have reported similar trends in compressive strength reduction with the incorporation of porous materials such as lightweight aggregates into mortar. Therefore, the porous structure of biochar has been identified as a contributing factor to the observed decrease in compressive strength, emphasising the importance of considering material characteristics when designing mortar mixtures.

It is important that, as the sand replacement percentage exceeded 40 %, the compressive strength values fell below the minimum requirements (20 MPa) outlined in BS EN 197-1 (British Standard Institution, 2011) for traditional mortar walls and columns. This emphasises the critical threshold beyond which the mixture may no longer meet the established standards for structural applications. On the other hand, the compressive strength measurements after 120 days of curing revealed a different aspect of the material's behaviour. The results indicated an improvement in compressive strength, with the sample at 50 % replacement exhibiting a notable increase from 15.91 MPa to 30.95 MPa. This phenomenon suggests that, over time, the mortar matrix undergoes changes that positively influence its mechanical properties. These findings could suggest a dynamic interaction between biochar and the mortar matrix, where long-term curing may contribute to enhanced bonding and mechanical performance. However, as stated earlier testing on biochar pozzolanic activities and XRD pattern of the resulted mixes indicated that biochar did not contribute to improving the compressive strength of the mortar.

Table 5: Thermal and mechanical properties of highest loading achieved in PCM-mortar literature studies, where $\Delta H_{f,\ PCM}$ is PCM Heat of Fusion (J/g); $\Delta H_{f,\ Co}$ is Composite Heat of Fusion (J/g); $T_{pc,\ Co}$ is Composite Phase Change Temperature (°C); σ_{comp} is Compressive Strength (MPa) and σ_{flex} is Flexural Strength (MPa).

PCM	Carrier Material	Building Material	$\Delta H_{f,\ PCM}$	$\Delta H_{f,\ Co}$	$T_{pc,\ Co}$	σ_{comp}	σ_{flex}	Reference
Octadecane	Biochar	Mortar	227.00	116.00	23.00	23.63	5.39	This study
RT18HC	Aerated Concrete	Mortar	195.00	75.00	18.00	25.90	5.39	(Wadee, et al., 2022)
RT22HC			118.00	50.20	22.00	23.98	5.28	
RT27HC			158.00	51.30	25.00	28.07	5.93	

Paraffin	Hydrophobic Expanded Perlite	Cement Mortar	133.30	12.15	19.20	7.53	-	(Jay, et al., 2015)
Paraffin	Graphite Flakes	Cement Mortar	248.80	135.80	28.32	14.20	4.10	(Zhang, et al., 2016)
Micro-encapsulated Paraffin	-	Lime Mortar	205.00	-	26.97	4.10	-	(Pavlík, et al., 2014)
Paraffin	Expanded Graphite	Cement Mortar	209.30	183.02	28.80	5.10	2.01	(Li, et al., 2013)
Paraffin	Expanded Perlite	Clay Geopolymer Mortar	135.46	96.77	38.21	8.00	-	(Wang, et al., 2016)
Micro-encapsulated Paraffin	-	Mix of Lime, Cement, And Gypsum	135.00	-	23.00	4.00	-	(Lucas, et al., 2013)
Micro-encapsulated Paraffin	-	Concrete, Mortar	187.50	-	28.00	34.40	3.90	(Lecompte, et al., 2015)
Micro-encapsulated Paraffin	Graphite Flakes	Cement Mortar	248.80	126.00	28.00	48.95	9.50	(Cui, et al., 2015)
Paraffin	Expanded Perlite	Cement Mortar	122.05	128.46	47.00	16.58	-	(Sun & Wang, 2015)

Similar observations of improved compressive strength over extended curing periods have been reported in studies such as the work of Hamada et al. who investigated impact of different curing method on the compressive strength of mortar (Hamada, et al., 2022). They

found that factors such as curing time, heat and pressure can improve the compressive strength of a mortar mix.

The observed reduction in compressive strength raises important considerations for real-world applications. While the incorporation of PCM-biochar may offer environmental benefits and improved thermal properties, it is crucial to assess the trade-offs in terms of structural performance. The results suggest that careful control of the PCM-biochar content is necessary to balance environmental goals with the mechanical requirements of the mortar.

When comparing the PCM-Biochar-Mortar composite with other trial composites listed in Table 5, it is evident that the PCM-biochar in mortar exhibits favourable results. The only exception is the work of Wadee et al. (Wadee, et al., 2022), where the use of lightweight aggregates resulted in higher compressive and flexural strengths. This superiority is attributed to the higher granularity index of lightweight aggregates in comparison with biochar (The grindability index is a measure of how easily a material can be ground into smaller particles and is highly correlated with strength) (Speight, 2019). However, the use of biochar presents distinct advantages over average lightweight aggregates due to its lower biogenic carbon content. This characteristic makes biochar a more sustainable and environmentally friendly option. The reduced biogenic carbon footprint of biochar highlights its potential as a preferable choice, especially in the context of promoting eco-friendly construction practices.

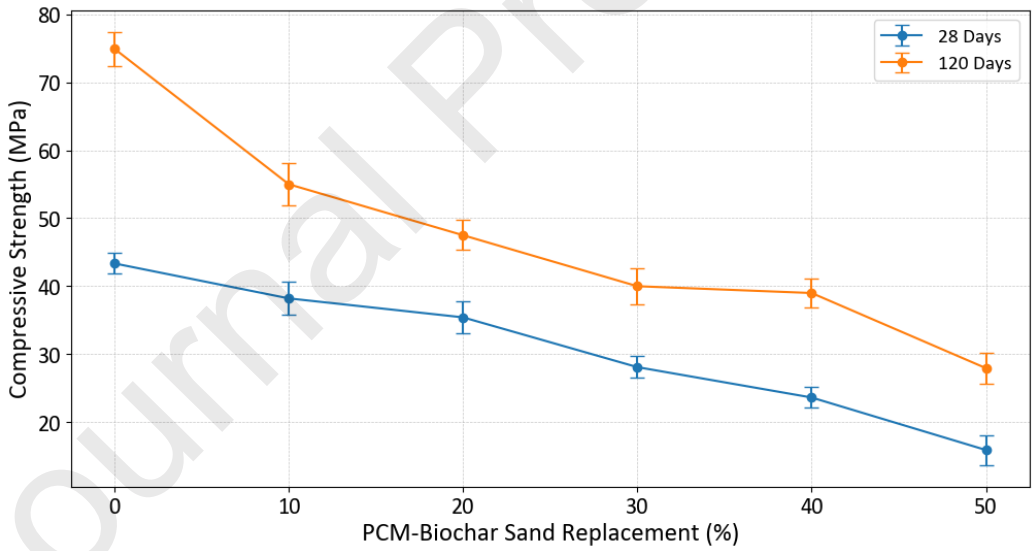

Fig. 17: Shows compressive strength (MPa) after 28 days and 120 days of curing Vs PCM-biochar for replacement percentages.

Mortar flexural strength

Similar to compressive strength, the flexural strength results indicate a decrease in resistance with increased PCM-biochar loading. This reduction is not significantly detrimental to the use of mortar in general construction, but there was a decrease of 46.08 % in flexural strength at

a 50 % PCM-biochar loading. The standard mortar sample had an average flexural strength of 8.16 ± 0.48 MPa. The decrease in flexural strength signifies the trade-off associated with the incorporation of PCM-biochar particles. Comparing the flexural strength data with the previously discussed compressive strength results, it is evident that both mechanical properties exhibit a reduction with increased PCM-biochar loading. Despite the initial reduction observed at 28 days see Fig. 18, the flexural strength shows signs of improvement over the extended curing period (Joshua, et al., 2018). Which is also a result of prolonged curing time. This correlation reinforces the need for a balanced approach when incorporating PCM-biochar into mortar formulations, considering both compressive and flexural performance.

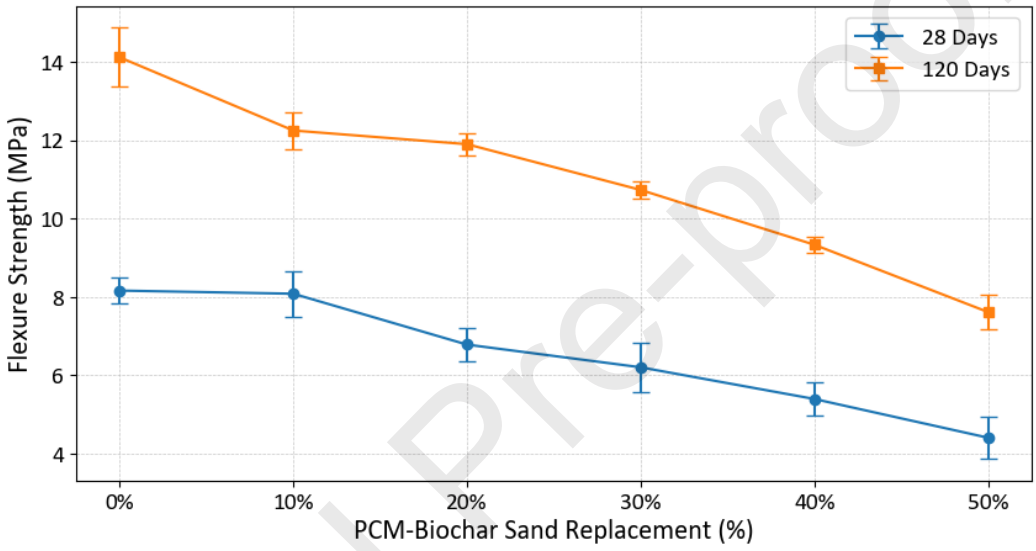

Fig. 18: Flexure strength after 28 days and 120 days of curing

Density, porosity and water absorption of mortars samples

Density of the mortar samples showed a decrease when increasing PCM-biochar particles loading. The addition of PCM-biochar to mortar sample results in a decrease in density from 2092.96 kg.m^{-3} for 0 % PCM-biochar particles replacement to 1661.18 kg.m^{-3} at 50 % PCM-biochar particles. A comparison of the density results with compressive strength at 28 days, clearly showed a correlation between the decrease in density and the observed decrease in the compressive strength. Furthermore, when the results from the density, workability, porosity, and water absorption measurements were analysed together a trend was observed. Fig. 19 shows the bulk density, total porosity and water absorption for the control mortar and mortar samples containing up to 50% PCM-biochar particles. The increase in the porosity of the cement mortar, leads to an increase in water absorption and decrease in bulk density. In addition to these results, several studies have concluded that an increase in porosity can

decrease the bulk dry density of cement mortar samples (Jayalath, et al., 2016) (Shima Pilehvar a b, et al., 2017).

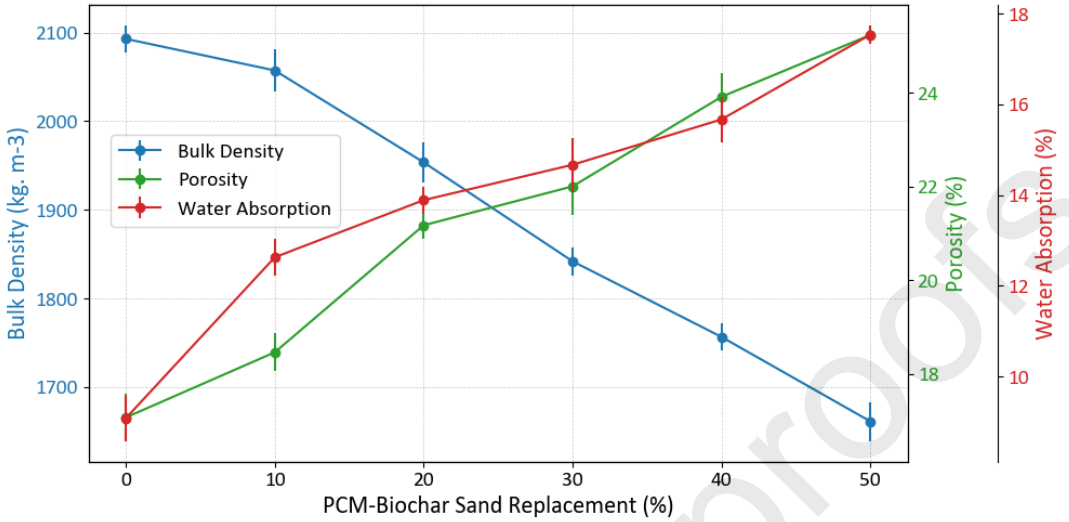

Fig. 19: Bulk density, porosity, and water absorption measurements of PCM-biochar mortar mixes

Porosity is also an important physical characteristic for the durability of cement mortars. The size, distribution and connectivity of the pore matrix are contributing factors to the permeability of the cement mortars and can be a defence against environmental agents (Li, et al., 2022). The results shown in Fig. 19 show a similar trend for porosity and water absorption. As the number of PCM-biochar particles increased, the porosity and water absorption also increased. For instance, the porosity of the samples at 0 % PCM-biochar particles increased from 17.07 % to approximately 25.23 % at 50 % PCM-biochar particles. The water absorption for the mortar mix at 0 % PCM-biochar particles replacement increased from 9.08 % to 17.54 % at 50 % PCM-biochar particles. This increase is mainly due to the replacement of sand with porous biochar as well as the reduced workability of the mortar mix as result of adding PCM-biochar particles.

Thermal conductivity and heat capacity of cement mortar samples

The energy consumption of a building is significantly influenced by heat loss through construction materials (Kumar, et al., 2023). Evaluating the heat transfer within materials, specifically through conduction, involves testing thermal conductivity. The thermal conductivity, and volumetric heat capacity of materials measurements were conducted at a temperature above the phase change temperature of the PCM at 28 °C, ensuring that the PCM was in its liquid phase. Fig. 20 shows the cross section of the PCM-biochar loaded cement mortar at different sand replacement. This indicates an even distribution of the PCM-biochar loaded particles within the cement samples. This is of important when conducting thermal

testing, as a homogeneous sample is required in order to obtain reliable data from the HotDisk thermal analyser.

Fig. 20: Cross section of the PCM-biochar loaded cement at different sand replacement.

Fig. 19 illustrates the impact of varying the amount of PCM-biochar particles on the thermal conductivity and heat capacity of PCM-biochar mortar mixes. Notably, the thermal conductivity of mortars containing PCM-biochar granules exhibited a significant decrease when increasing the percentage of PCM-biochar granules. For instance, for the control sample with 0% replacement, the average thermal conductivity was 2.81 (±0.05) W. mK^{-1}. Conversely, the mortar samples with 10 %, 20 %, 30 %, 40 %, and 50 % sand replacement displayed thermal conductivities of 2.42 (±0.04) $W.m^{-1}K^{-1}$, 2.02 (±0.03) $W.m^{-1}K^{-1}$, 1.9 (±0.06) $W.m^{-1}K^{-1}$, 1.6 (±0.05) $W.m^{-1}K^{-1}$, and 1.4 (±0.02) $W.m^{-1}K^{-1}$, respectively. This corresponds to percentage reductions of 13.87%, 28.11%, 32.38%, 43.06%, and 50.17% in thermal conductivity at each sand replacement level. The decrease in thermal conductivity is caused by the increased porosity and any trapped air within the biochar pores contributes to this reduction. Compared to octadecane PCMs (with a thermal conductivity of 0.153 $W.m^{-1}K^{-1}$ (Yu, et al., 2014)), the cement mortar specimens (2.81 W. $m^{-1}K^{-1}$) exhibited a decreased thermal conductivity as the amount of PCM-biochar granules increased. While a lower thermal conductivity is advantageous for insulation, it poses challenges for the phase change properties of PCM and the efficiency of heat transfer during phase transition.

This study's findings aligns with reports from other researchers attempting to incorporate PCMs into Portland cement (Jayalath, et al., 2016), (Shima Pilehvar a b, et al., 2017), (Cao, et al., 2017).

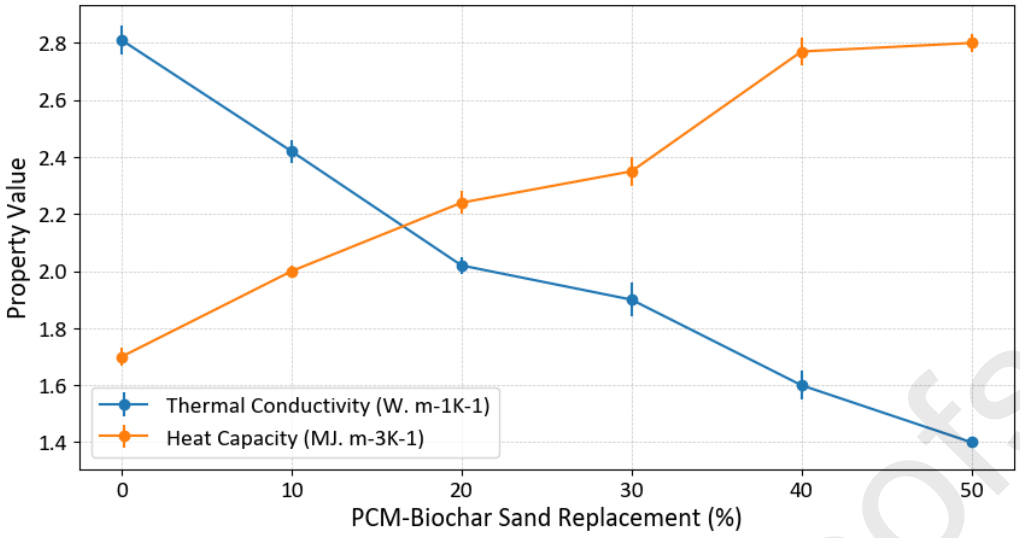

Fig. 21: Thermal conductivity measurement ($W.m^{-1}K^{-1}$) and specific heat capacity ($MJ.m^{-1}K^{-1}$) of different PCM-biochar mortar mixes.

The volumetric heat capacity of PCM-biochar mortar rises with increasing PCM-biochar granules content, as evidenced in Fig. 21. Using the measured thermal diffusivity of PCM-biochar mortar mixes the volumetric heat capacity was calculated. The volumetric heat capacity of the standard mortar mix with 0 % PCM-biochar loading measurement was 1.7 (±0.04) $MJ\cdot m^{-3}K$ while the measured volumetric heat capacity of the PCM-biochar mortar mix at 50 % loading was 2.8 (±0.02) $MJ\cdot m^{-3}K$. As 50 % loading PCM-biochar mortar was the maximum loading investigated in this study, thus the maximum increase in volumetric specific heat capacity was 64.70 %. However, the maximum practical increase of volumetric specific heat capacity is 62.94 % at 40 % sand replacement as this gives us a compressive strength above the minimum requirement of BSI as previously discussed in section 0. The high heat capacity is useful for thermal energy storage applications as they allow for thermal energy to be stored and used later. Hence, samples with higher loading of PCM-biochar particles are more desirable for thermal storage applications in built environment.

Compressive strength, flexural strength, and density of gypsum samples

The compressive strength of the different PCM-biochar gypsum samples listed in Table 2 was measured and the results are illustrated in Fig. 22. The addition of PCM-biochar particles to gypsum reduces the compressive strength of the material. The compressive strength of the control sample with 0 % PCM-biochar particles dropped from 4.05 MPa to 2.71 MPa when PCM-biochar particles loading reached 50%, which translates to a reduction of 33.09% in compressive strength. Although the addition of PCM-biochar particles reduced the compressive strength of the gypsum samples, the resulting compressive strength value still lies above the minimum mechanical requirement of 2 MPa given in BS EN 13279-1. As with the cement mortar samples, the reduced compressive strength of the gypsum mixes can also

be attributed to the introduction of a material that is less dense and more porous than gypsum.

The flexural strength data for gypsum with PCM-biochar at different loading percentage are also shown in Fig. 22. The mixes followed the same general trend shown in the compressive strength measurements. The flexural strength declined as the PCM-biochar loading increased. At 50 % PCM-biochar particles loading, the flexural strength decreased by approximately 15% from 1.68 (±0.03) MPa at 0 % PCM-biochar loading to about 1.43 (±0.02) MPa. The reduction in flexural strength also stems from the incorporation of more porous material, and although the incorporation of PCM-biochar into gypsum reduces its flexural strength this reduction should not cause any impracticality when using this material in general construction since it is still above the standardised minimum required value of 1 MPa.

Finally, densities of the manufactured gypsum samples were also measured, and the results are listed in Fig. 22. The density measurements showed a descending trend complementing the results from the compressive strength and flexural strength tests. The reduced density again can only be explained by the addition of more PCM-biochar particles, which is a porous material that resulted in a reduced density and decreased strength.

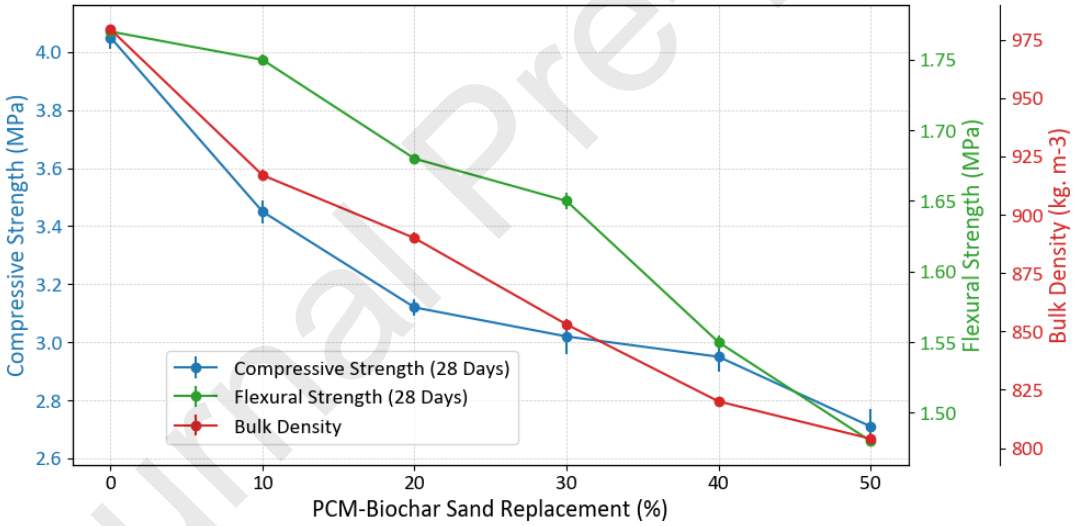

Fig. 22: Compressive and flexural strength and bulk density of PCM-biochar gypsum mixes

Thermal conductivity and heat capacity of gypsum samples

The effect of adding PCM-biochar granules into gypsum samples at different replacement percentages is shown in Fig. 23. Overall, the thermal conductivity of gypsum samples containing PCM-biochar granules decreases with the increase of PCM-biochar granules. The thermal conductivity decreased from 0.301 (±0.004) $W.m^{-1}K^{-1}$ at 0% PCM-biochar granules to approximately 0.252 (±0.002) $W{\cdot}m^{-1}K^{-1}$ at 50% PCM-biochar granules, which is a 16 % reduction. This reduction can be attributed to several factors. Biochar's inherent insulating properties act as a thermal barrier, impeding heat transfer, while the presence of PCMs within

the granules contributes to lower thermal conductivity during phase transitions. Increased porosity from the granules introduces air gaps that further give insulation properties to the material. The potential mismatch in thermal properties and the unique surface characteristics of biochar may also play a role in scattering and reflecting thermal energy. The observed lower thermal conductivity of the gypsum mix with PCM-biochar granules suggests its potential suitability for applications in the built environment, where enhanced thermal insulation is desirable.

The volumetric heat capacity of the mix was also studied, and the results from the addition of PCM-biochar granules into gypsum are listed in Fig. 23. As in the case of the cement mortars, the heat capacity value was found to rise with the increase of the PCM-biochar content in the gypsum mixes. For instance, at 0% PCM-biochar loading the heat capacity of the materials was 0.97 (±0.03) $MJ{\cdot}m^{-3}K^{-1}$ and when the PCM-biochar loading increased to 10% and then 50% the heat capacity rose to 1.14 (±0.04) $MJ{\cdot}m^{-3}K^{-1}$ and 1.68 (±0.05) $MJ{\cdot}m^{-3}K^{-1}$, respectively. Consequently, samples featuring the highest replacement percentage of PCM-biochar loaded granules, and thereby demonstrating the highest heat capacity, emerge as particularly suitable for integration into building materials designed for thermal energy storage, especially in the retrofitting of existing low energy-efficient buildings.

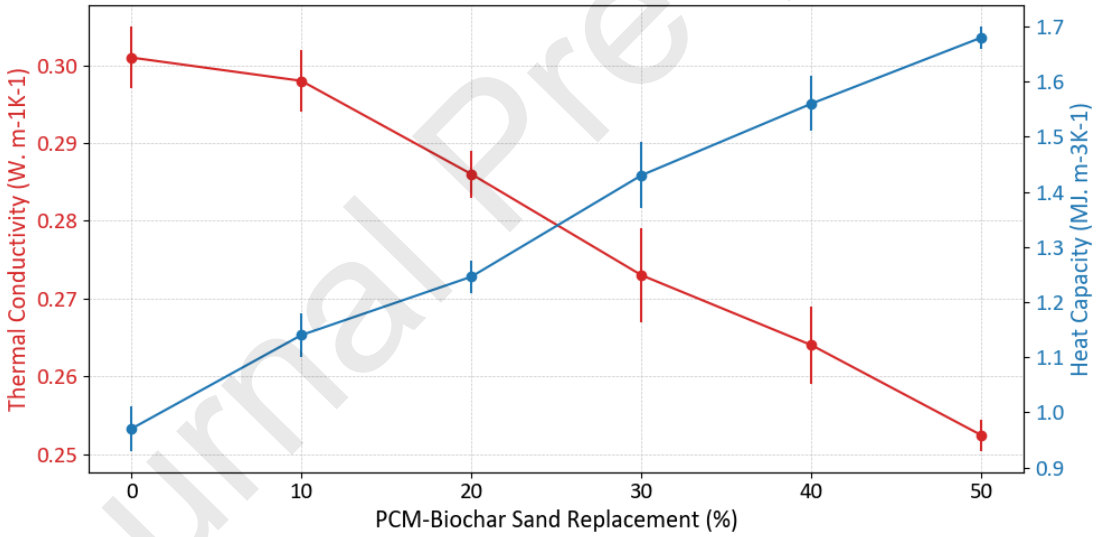

Fig. 23: Thermal properties vs different PCM-biochar loading into gypsum mix.

Conclusions

The impregnation of octadecane PCM into biochar particles was systematically explored, comparing immersion and vacuum absorption methods. Notably, latter method, vacuum impregnation, exhibited superior results, yielding a 34.48 % higher loading at a PCM-biochar ratio of 2.5:1.0. The selected optimum ratio, coupled with specific conditions of 2 bar pressure and 70 °C, demonstrated a favourable impregnation level of 62.21 %. With this method, a latent heat energy of 116.7 $J{\cdot}\ g^{-1}$ was achieved which surpassed other methods reported in

the literature. Hence, showcasing its potential for thermal energy storage in building materials. Further thermal analysis via TGA confirmed the composite's stability at high temperatures, while accelerated DSC validated its phase change capability and stability over 300 cycles. SEM, SAXS, ^{1}H NMR and PXRD analyses confirmed PCM retention within biochar pores, with dipole-dipole interaction between biochar and PCM. Additionally, the pozzolanic activity of biochar, attributed to its chemical composition, was evaluated using Chapelle test measurements. The biochar pozzolanic index was found to be below the minimum threshold of 1000 ($Ca(OH)_2$/biochar). This finding was corroborated by XRD pattern analysis. These results help in understanding the impact of incorporating PCM-biochar into mortar. Specifically, they show an initial reduction of over 45% in mortar strength during the first 28 days of curing. The incorporation of PCM-biochar particles into mortar and gypsum revealed comprehensive outcomes crucial for practical applications.

In terms of mortar workability, the study demonstrated a consistent reduction when increasing PCM-biochar particles, emphasising the impact of biochar's porous nature. Mortar calorimetry results indicated no notable delay in hydration, and compressive strength evaluations highlighted a reduction after 28 days, emphasising the challenge posed by the porous structure of biochar. However, an interesting reversal was observed after 120 days, suggesting dynamic interactions between biochar and the mortar matrix. The reduction in compressive and flexural strength and density, accompanied by increased porosity and water absorption, reinforced the trade-off associated with incorporating PCM-biochar particles. Notably, the study showcased a significant decrease in thermal conductivity with increasing PCM-biochar granules, offering enhanced insulation potential. Despite the reduction in mechanical properties, the volumetric heat capacity of PCM-biochar mortar increased, presenting an opportunity for efficient thermal energy storage in the built environment.

For gypsum samples, the addition of PCM-biochar led to a reduction in compressive and flexural strength, as well as density. However, these reductions remained within acceptable limits for practical use. Thermal conductivity declined when PCM-biochar content increased, indicating improved insulation. The study also highlighted an increase in volumetric heat capacity with PCM-biochar loading, affirming the potential of these samples for thermal energy storage applications in building materials. The findings underscore the need for a balanced approach, considering both mechanical performance and thermal properties, when incorporating PCM-biochar particles into construction materials.

Acknowledgement

The authors greatly appreciate the financial support provided by Engineering and Physical Sciences Research Council (EPSRC) of UK (Grant No.: EP/T518013/1).

References

Aguayo, M. et al., 2017. Porous inclusions as hosts for phase change materials in cementitious composites: Characterization, thermal performance, and analytical models.. *Constr. Build. Mater.,* Volume 134, pp. 574-584.

Akinyemi, B. A. & Adesina, A., 2020. Recent advancements in the use of biochar for cementitious applications: A review. *Build. Eng.,* Volume 32, p. 101705.

Al-Yasiri, Q. & Szabó, M., 2021. Incorporation of phase change materials into building envelope for thermal comfort and energy saving: A comprehensive analysis. *Build. Eng.,* Volume 36, p. 102122.

Ashraf, A., 2014. *Thermal Conductivity Measurement by Hot Disk Analyser.* [Online]
Available at:
https://www.researchgate.net/publication/271840994_Thermal_Conductivity_Measurement_by_Hot_Disk_Analyser
[Accessed 28 10 2023].

Atinafu, D. G., Chang, S. J., Kim, K.-H. & Kim, S., 2020. Tuning surface functionality of standard biochars and the resulting uplift capacity of loading/energy storage for organic phase change materials. *Chem. Eng.,* Volume 394, p. 125049.

Azzi, E. S., Karltun, E. & Sundberg, C., 2019. Prospective Life Cycle Assessment of Large-Scale Biochar Production and Use for Negative Emissions in Stockholm. *Environ. Sci. Tech.,* Volume 53, pp. 8466-8476.

Bernal, S. A. et al., 2017. Characterization of supplementary cementitious materials by thermal analysis. *Mater. Struct.,* Volume 50, p. 26.

Bézard, D., 2002. *Metakaolin - measuring the total quantity of fixed Calcium Hydroxide (Chapelle test modified) Referring to the French norm NF P 18-513.* [Online]
Available at: https://metakaolin.info/quality-criteria/chapelle-test.html
[Accessed 15 10 2023].

British Standard Institution, 1998. *Tests for mechanical and physical properties of aggregates. Determination of loose bulk density and voids,* London: BSI.

British Standard Institution, 2011. *BS EN 197-1: 2011 Cement - Composition, specifications and conformity criteria for common cements,* London: BSI.

British Standard Institution, 2013. *Aggregates for concrete,* London: BSI.

British Standard Institution, 2022. *Tests for mechanical and physical properties of aggregates - Determination of particle density and water absorption,* London : BSI.

British Standards Institution , 1999. *Methods of test for mortar for masonry - Determination of dry bulk density of hardened mortar BS EN 1015-10:1999,* London: BSI.

British Standards Institution , 2009. *BS EN 13279-1:2008 Gypsum binders and gypsum plasters - Definitions and requirements,* London: BSI.

British Standards Institution, 2016. *Methods of testing cement Determination of strength BS EN 196-1,* London: BSI.

Camp, C., 2017. *Relative Density and Absorption of Aggregate,* Memphis: University of Memphis..

Cao, V. D. et al., 2017. Microencapsulated phase change materials for enhancing the thermal performance of Portland cement concrete and geopolymer concrete for passive building applications. *Energy Convers. Manag.,* Volume 133, pp. 56-66.

Cui, H. et al., 2015. Study on functional and mechanical properties of cement mortar with graphite-modified microencapsulated phase-change materials. *Energy and Build.,* Volume 105, pp. 273-284.

Cui, Y., Xie, J., Liu, J. & Pan, S., 2015. Review of phase change materials integrated in building walls for energy saving. *Procedia Eng.,* Volume 121, pp. 763-770.

Dehdezi, P. K., Hall, M. R., Dawson & R., A., 2013. Thermal, mechanical and microstructural analysis of concrete containing microencapsulated phase change materials. *Int. J. Pavement Eng.,* 14(5), p. 449.

Department for Business, Energy & Industrial Strategy (BEIS), 2022. *Energy Consumption in the UK (ECUK) 1970 to 20221.* [Online]
Available at:
https://assets.publishing.service.gov.uk/government/uploads/system/uploads/attachment_data/file/1110483/Energy_Consumption_in_the_UK_2022_10102022.pdf
[Accessed 25 08 2024].

Donatello, S., Tyrer, M. & Cheeseman, C., 2010. Comparison of test methods to assess pozzolanic activity. *Cem. Concr. Compos.,* 32(2), pp. 121-127.

Eddhahak-Ouni, A., Drissi, S., Colin, J. & Caré, S., 2014. Effect of Phase Change Materials (PCMs) on the hydration reaction and kinetic of PCM-mortars. *Therm. Anal. Calorim.,* 117(2), pp. 537-545.

Elango, K., Sanfeer, J., Gopi, R. & A. Shalini c, R. S. a. L. P. d., 2021. Properties of light weight concrete – A state of the art review. *Mater. Today Proc.,* Volume 46, pp. 4059-4062.

Epp, J., 2016. X-ray diffraction (XRD) techniques for materials characterization. In: 4, ed. *Materials Characterization Using Nondestructive Evaluation (NDE) Methods.* 4 ed. s.l.:Woodhead Publishing, pp. 81-124.

Fabiani, C., Santini, C., Barbanera, M. & Giannoni, T., 2023. Phase change materials-impregnated biomass for energy efficiency in buildings: Innovative material production and multiscale thermophysical characterization. *Energy Storage,* Volume 58, p. 106223.

Faden, M. et al., 2019. Review of Thermophysical Property Data of Octadecane for Phase-Change Studies. *Materials ,* 12(18), p. 2974.

G, D. et al., 2020. Tuning surface functionality of standard biochars and the resulting uplift capacity of loading/energy storage for organic phase change materials. *Chem. Eng.,* Volume 394, p. 125049.

Giro-Paloma, J., Martínez, M., Cabeza, L. & Fernández, A., 2016. Types, methods, techniques, and applications for microencapsulated phase change materials (MPCM): A review. *Renew. Sustain. Energy Rev.,* Volume 53, pp. 1059-1075.

Haddad, L. D. d. O. et al., 2020. Influence of particle shape and size distribution on coating mortar properties. *Mater. Res. Technol.,* 9(4), pp. 9299-9314.

Hadjipanayis, G. et al., 1992. Preparation of Fine Particles. *Magn. Prop. Fine Particles.,* pp. 35 - 46.

Haider, M. Z. et al., 2022. Enhancing the compressive strength of thermal energy storage concrete containing a low-temperature phase change material using silica fume and multiwalled carbon nanotubes. *Constr. Build. Mater.,* Volume 314, p. 125659.

Hamada, H. et al., 2022. Influence of different curing methods on the compressive strength of ultra-high-performance concrete: A comprehensive review. *Case Stud. Constr. Mater.,* Volume 17, p. e01390.

Hao, R., Li, X., X, P. & Liu, Q., 2022. Thermal activation and structural transformation mechanism of kaolinitic coal gangue from Jungar coalfield, Inner Mongolia, China. *Appl. Clay Sci.,* Volume 223, p. 106508.

Harini, M., Shaalini, G. & Dhinakaran, G., 2012. Effect of size and type of fine aggregates on flowability of mortar. *KSCE J. Civ. Eng.,* 16(1), pp. 163-168.

Hewlett, P. C., Sims, I. & Brown, B., 1998. 16 - Concrete Aggregates. In: 4, ed. *Lea's Chemistry of Cement and Concrete.* Oxford: Elsevier Ltd, pp. 907-1015.

Huang, Y., Stonehouse, A. & Abeykoon, C., 2023. Encapsulation methods for phase change materials – A critical review. *Int. J. Heat Mass Transf.,* Volume 200, p. 123458.

Hunger, M. et al., 2009. The behavior of self-compacting concrete containing micro-encapsulated Phase Change Materials. *Cem. Concr. Compos.,* 31(10), pp. 731-743.

Hussein, M. Z., Khadiran, T., Zainal, Z. & Rusli, R., 2015. Properties of N-Octadecane-Encapsulated Activated Carbon Nanocomposite for Energy Storage Medium: The Effect of Surface Area and Pore Structure. *Aust. J. Basic Appl. Sci.,* 9(8), pp. 82-88.

Hussein, M. Z., Khadiran, T., Zainal, Z. & Rusli, R., 2015. Properties of N-Octadecane-Encapsulated Activated Carbon Nanocomposite for Energy Storage Medium: The Effect of Surface Area and Pore Structure. *AJBAS,* 9(8), pp. 82-88.

Hussein, M. Z., Nicholas, A. F., Zainal, Z. & Khadiran, T., 2020. The effect of surface area on the properties of shape-stabilized phase change material prepared using palm kernel shell activated carbon. *Sci. Rep.,* Volume `0, p. 15047.

Jawaid, M. & Khan, M. M., 2018. *Polymer-Based Nanocomposites for Energy and Environmental Applications,* Cambridge: Woodhead Publishing: Sawston.

Jayalath, A., Nicolas, R. S. & Massoud Sofi a, R. S. b. T. N. a. L. A. a. P. M. a., 2016. Properties of cementitious mortar and concrete containing micro-encapsulated phase change materials. *Constr. Build. Mater.,* Volume 120, pp. 408-417.

Jay, S. et al., 2015. A novel paraffin/expanded perlite composite phase change material for prevention of PCM leakage in cementitious composites. *Appl. Energy,* Volume 157, pp. 85 - 94.

Jeon, I. K. et al., 2023. Effects of shape-stabilized phase change materials in cementitious composites on thermal-mechanical properties and economic benefits. *Appl. Therm. Eng.,* 25(219), p. 119444.

Jeon, J. et al., 2019. Characterization of biocomposite using coconut oil impregnated biochar as latent heat storage insulation. *Chemosphere,* Volume 236, p. 124269.

Jeon, J. et al., 2019. Latent heat storage biocomposites of phase change material-biochar as feasible eco-friendly building materials. *Environ. Res.,* Volume 172, pp. 637-648.

Johansson, P., Parberit, R. & Ojerborn, J., 2016. *Evalution of PCM activiation using changes in physical properties during phase transition for visualisation of passive building envelope technologies.* Incheon, 9th International Conference on Indoor Air Quality Ventilation & Energy Conservation In Buildings (IAQVEC 2016).

Joshua, O. et al., 2018. Investigating for pozzolanic activity in the blend of ground glass waste with cement for sustainable concrete. *Int. J. Mech. Eng. Technol.,* 6(9), pp. 808-816.

Kalnaes, S. E. & Jelle, B. P., 2015. Phase change materials and products for building applications: A state-of-art-review and future research opportunities. *Energy and Build.,* Volume 94, pp. 150-176.

Karaipekli, A. & Sarı, A., 2009. Capric–myristic acid/vermiculite composite as form-stable phase change material for thermal energy storage. *Sol. Energy,* 83(3), pp. 323-332.

Katish, M., Allen, S., Squires, A. & Ferrandiz-Mas, V., 2024. Thermal stability of organic phase change materials (PCMs) by accelerated thermal cycling technique. *Thermochimica Acta,* Volume 737, p. 179771.

Kenisarin, M. M., 2014. Thermophysical properties of some organic phase change materials for latent heat storage. A review. *Sol. Energy,* Volume 107, pp. 553-575.

Konuklu, Y., Ostry, M., Paksoy, H. & Charvat, P., 2015. Review on using microencapsulated phase change materials (PCM) inbuilding applications. *Energy Build.,* Volume 106, pp. 134 - 155.

Kosmatka, S. H., Kerkhoff, B. & Panarese, W. C., 2002. *Design and Control of Concrete Mixtures Edition: 14th.* North Dakota: Portland Cement.

Kumar, D., Alam, M. & Doshi, A. J., 2023. Investigating the Influence of Thermal Conductivity and Thermal Storage of Lightweight Concrete Panels on the Energy and Thermal Comfort in Residential Buildings. *Build.,* 13(3), p. 720.

Lecompte, T. et al., 2015. Mechanical and thermo-physical behaviour of concretes and mortars containing phase change material. *Energy and Build.,* Volume 94, pp. 52-60.

Leussa, C. C. T. et al., 2020. Pozzolanic activity of kaolins containing aluminum hydroxide. *Sci. Rep.,* Volume 10, p. 13230 .

Li, M., Wu, Z. & Tan, J., 2013. Heat storage properties of the cement mortar incorporated with composite phase change material. *Appl. Energy,* Volume 103, pp. 393-399.

Ling, T.-C. & Poon, C.-S., 2013. Use of phase change materials for thermal energy storage in concrete: An overview. *Constr. Build. Mater.,* Volume 46, pp. 55 - 62.

Li, P. et al., 2022. Experimental study and analytical model for the pore structure of epoxy latex-modified mortar. *Sci. Rep.,* Volume 12, p. 5822.

Liu, F., Wang, J. & Qian, X., 2017. Integrating phase change materials into concrete through microencapsulation using cenospheres. *Cem. Concr. Compos.,* Volume 80, pp. 317 - 325.

Liu, Y. et al., 2021. Tailored design of food waste hydrochar for efficient adsorption and catalytic degradation of refractory organic contaminant. *Clean. Prod.,* Volume 310, p. 127482.

Lucas, S., Ferreira, V. & Aguiar, J. L. B. d., 2013. Latent heat storage in PCM containing mortars - Study of microstructural modifications. *Energy Build.,* Volume 66, pp. 724-731.

Majumder, R., 2020. *Vacuum impregnation method for Aluminium castings shoulders environmental responsibility.* [Online]
Available at: https://www.alcircle.com/news/vacuum-impregnation-method-for-aluminium-castings-shoulders-environmental-responsibility-57806
[Accessed 31 10 2023].

Martín, C. et al., 2021. Pozzolanic activity quantification of hollow glass microspheres. *Cem. Concr. Compos.,* Volume 118, p. 103981.

Mehta, P. a. P. M., 2006. *Concrete: Microstructure, properties and materials.* London: McGraw-Hill.

Pavlík, Z. et al., 2014. Experimental Investigation of the Properties of Lime-Based Plaster-Containing PCM for Enhancing the Heat-Storage Capacity of Building Envelopes. *Int. J. Thermophys,* Volume 35, p. 767–782.

Pielichowski, K. & Pielichowska, K., 2014. Phase change materials for thermal energy storage. *Prog. Mater. Sci.,* Volume 65, pp. 67-123.

Qi, T. et al., 2021. Theory, Predictive Hydration Model of Portland Cement and Its Main Minerals Based on Dissolution Theory and Water Diffusion. *Materials,* 14(3), p. 595.

Renforth, P., 2022. *Phil Renforth on Carbon Sequestration.* [Online]
Available at: https://www.geologybites.com/phil-renforth
[Accessed 04 11 2023].

Roussel, N., 2011. *Understanding the Rheology of Concrete.* 1st ed. Cambridge: Elsevier.

S. Donatello, M. T. & Cheeseman, C., 2010. Comparison of test methods to assess pozzolanic activity. *Cem. Concr. Compos.,* 32(2), pp. 121-127.

S. Schaefer a, A. J. a. b. G. S. P. G. et al., 2020. Oxygen-promoted hydrogen adsorption on activated and hybrid carbon materials. *Int. J. Hydrog. Energy.,* 55(45), pp. 30767-30782.

Sani, A. K., Olawoore, I. O. & Singh, R. M., 2021. Assessment of impregnating phase change materials into lightweight aggregates for development of thermal energy storage aggregate composites. *Constr. Build. Mater.,* Volume 305, p. 124683.

Santos, A. A. M. d. & Cordeiro, G. C., 2021. Investigation of particle characteristics and enhancing the pozzolanic activity of diatomite by grinding. *Mater. Chem. Phys.,* Volume 270, p. 124799.

Sarı, A., Bicer, A., Karaipekli, A. & Al-Sulaiman, F., 2018. Preparation, characterization and thermal regulation performance of cement based-composite phase change material. *Sol. Energy Mater. Sol. Cells,* Volume 174, pp. 523-529.

Scrivener, K. L., Juilland, P. & Monteiro, P. J., 2015. Advances in understanding hydration of Portland cement. *Cem. Concr. Res.,* 78(Part A), pp. 38-56.

Sedaghat, A. et al., 2014. Investigation of Physical Properties of Graphene-Cement Composite for Structural Applications. *Open J. Compos. Mater.,* Volume 2014, pp. 12-21.

Shaheen, S. M. et al., 2019. Wood-based biochar for the removal of potentially toxic elements in water and wastewater: a critical review. *Int. Mater. Rev.,* 64(4), p. 216–247.

Sharma, R., Jang, J.-G. & Hu, a. J.-W., 2022. Phase-Change Materials in Concrete: Opportunities and Challenges for Sustainable Construction and Building Materials. *Materials,* Volume 15, p. 335.

Shima Pilehvar a b, V. D. C. a. c. A. M. S., Valentini, L., Salvioni, D. & Matteo Magistri f, R. P. b. A.-L. K., 2017. Mechanical properties and microscale changes of geopolymer concrete and Portland cement concrete containing micro-encapsulated phase change materials. *Cem. Concr. Res.,* Volume 314-349, p. 100.

Skevi, L., Baki, V. A., Feng, Y. & Ke, M. V. a. X., 2022. Biomass Bottom Ash as Supplementary Cementitious Material: The Effect of Mechanochemical Pre-Treatment and Mineral Carbonation. *Materials,* Volume 15, p. 8357.

Speight, J. G., 2019. Handbook of Industrial Hydrocarbon Processes. In: *Chapter 5 - Hydrocarbons from coal.* s.l.:Elsevier, pp. 193-242.

Sukontasukkul, P. et al., 2020. Thermal storage properties of lightweight concrete incorporating phase change materials with different fusion points in hybrid form for high temperature applications. *Heliyon,* 6(9), p. E04863.

Sun, D. & Wang, L., 2015. Utilization of paraffin/expanded perlite materials to improve mechanical and thermal properties of cement mortar. *Constr. Build. Mater.,* Volume 101, Part 1, pp. 791-796.

United Nations Environment Programme, 2022. *CO2 emissions from buildings and construction hit new high, leaving sector off track to decarbonize by 2050: UN.* [Online]
Available at: https://www.unep.org/news-and-stories/press-release/co2-emissions-buildings-and-construction-hit-new-high-leaving-sector
[Accessed 11 10 2024].

Uthaichotirat, P. et al., 2020. Thermal and sound properties of concrete mixed with high porous aggregates from manufacturing waste impregnated with phase change material. *Build. Eng.,* Volume 29, p. 101111.

Wadee, A., Walker, P., McCullen, N. & Ferrandiz-Mas, V., 2022. Lightweight aggregates as carriers for phase change materials. *Constr. Build. Mater.,* Volume 360, p. 129390.

Wang, Z., Su, H., Zhao, S. & Zhao, N., 2016. Influence of phase change material on mechanical and thermal properties of clay geopolymer mortar. *Constr. and Build. Mater.,* Volume 120, pp. 329-334.

Weller, M., 2014. *Inorganic Chemistry.* 6th ed. Bath: Oxford University Press.

Yuqing Sun, X. X. M. H. et al., 2021. Roles of biochar-derived dissolved organic matter in soil amendment and environmental remediation: A critical review. *Chem. Eng.,* Volume 424, p. 130387.

Yu, S., Wang, X. & Wu, D., 2014. Microencapsulation of n-octadecane phase change material with calcium carbonate shell for enhancement of thermal conductivity and serving durability: Synthesis, microstructure, and performance evaluation. *Appl. Energy,* Volume 114, pp. 632-643.

Zhang, H. et al., 2016. A novel phase-change cement composite for thermal energy storage: Fabrication, thermal and mechanical properties. *Appl. Energy,* Volume 170, pp. 130 - 139.

Appendix

Table 6: Results of immersion method and vacuum impregnation of octadecane and biochar, the data represent an average of three replicas.

PCM-biochar(wt.%) Ratio	Octadecane Percentage Absorption (wt.%)	
	Immersion Method	Vacuum Impregnation
0.5:1.0	23.67 (±0.94)	27.19 (±0.13)
1.0:1.0	29.29 (±0.16)	36.67 (±0.33)
1.5:1.0	37.54 (±0.79)	45.21 (±0.25)
2.0:1.0	43.73 (±0.55)	57.04 (±0.34)
2.5:1.0	45.62 (±0.36)	61.35 (±0.29)
3.0:1.0	46.25 (±0.06)	62.21 (±0.11)

Table 7: Workability (mm) vs PCM replacement (%)

PCM Replacement	Workability (mm)
0%	21.10 ±0.05
10%	20.45 ±0.04
20%	19.94 ±0.056
30%	18.29 ±0.067
40%	18.01 ±0.012
50%	17.59 ±0.032

Table 8: Properties of PCM loaded mortar samples at different loading values.

PCM-biochar Sand Replacement	Porosity (%)	Bulk Density (kg. m^{-3})	Water Absorption (%)	Thermal conductivity ($W.m^{-1}.K^{-1}$)	Heat Capacity ($MJ.m^{-3}.K^{-1}$)
0%	17.07 (±1.01)	2092.96 (±13)	9.08 (±1.5)	2.81 (±0.05)	1.7 (±0.04)
10%	18.46 (±1.7)	2057.32 (±24.5)	12.63 (±2.4)	2.42 (±0.04)	2 (±0.04)
20%	21.17 (±2.1)	1953.59 (±23)	13.89 (±2.02)	2.02 (±0.03)	2.24 (±0.03)
30%	22 (±1.9)	1841.88 (±16)	14.67 (±1.6)	1.9 (±0.06)	2.35 (±0.06)
40%	23.91 (±2.1)	1756.53 (±15)	15.67 (±01.2)	1.6 (±0.05)	2.77 (±0.05)
50%	25.23 (±1.3)	1661.18 (±22)	17.54 (±1.2)	1.4 (±0.02)	2.8 (±0.02)

Table 9: Compressive strength and flexure strength results for cement mortar

PCM-biochar Sand Replacement	Compressive Strength at 28 Days	Compressive Strength at 120 days	Flexure Test at 28 days	Flexure Test at 120 days
0%	43.35 (±1.2)	74.92 (±2.5)	8.16 (±1.15)	14.12 (±0.76)
10%	38.21 (±2.4)	60 (±3.1)	7.08 (±1.42)	12.25 (±0.48)
20%	35.42 (±2.3)	57.5 (±2.2)	6.88 (±1.30)	11.90 (±0.28)
30%	28.1 (±1.6)	47 (±2.6)	6.2 (±1.62)	10.73 (±0.22)

40%	23.63 (±1.5)	43 (±2.1)	5.39 (±1.43)	9.33 (±0.19)
50%	15.91 (±2.2)	30.95 (±2.3)	4.4 (±1.54)	7.61 (±0.44)

Table 10: Compressive strength and flexural strength, density, and thermal properties for gypsum mix

PCM-biochar Addition Percentage	**Compressive strength (MPa) 28 Days**	**Flexural Strength (MPa) 28 Days**	**Bulk Density (kg. m^{-3})**	**Thermal conductivity ($W.m^{-1}.K^{-1}$)**	**Heat Capacity ($MJ.m^{-3}.K^{-1}$)**
0	4.05 (±0.04)	1.88 (±0.03)	979.5 (±1.5)	0.301 (±0.004)	0.97 (±0.03)
0.1	3.45 (±0.04)	1.77 (±0.04)	917 (±2.4)	0.288 (±0.004)	1.14 (±0.04)
0.2	3.12 (±0.03)	1.75 (±0.03)	890 (±2.3)	0.276 (±0.003)	1.246 (±0.03)
0.3	3.02 (±0.06)	1.65 (±0.06)	853 (±1.6)	0.253 (±0.006)	1.43 (±0.06)
0.4	2.95 (±0.05)	1.55 (±0.05)	820 (±1.5)	0.22 (±0.005)	1.56 (±0.05)
0.5	2.71 (±0.02)	1.43 (±0.02)	804 (±2.2)	0.204 (±0.002)	1.68 (±0.02)

Chapelle Test:

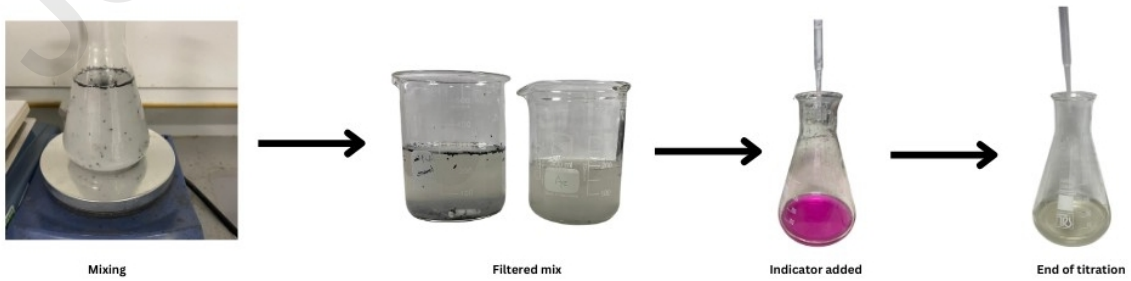

Fig. 24. Chapelle test steps using lab images.

Highlights

1. Vacuum impregnation achieves 62.21% Phase Change Materials (PCMs) loading.
2. Improved insulation and specific heat capacity in mortar and gypsum composites.
3. PCM-Biochar interaction validated through thorough analysis.
4. Maximum PCM loading of 40%; maintains mechanical properties of building materials.

CRediT author statement

Mohamed Katish: Conceptualisation; Methodology; Investigation; Visualisation and Writing - Original Draft **Stephen Allen**: Conceptualisation; Resources; Writing - Review and Editing; Supervision; Project Administration **Adam Squires**: Conceptualisation; Resources; Writing - Review and Editing; Supervision **Veronica Ferrandiz-Mas**: Conceptualisation; Resources; Supervision; Writing – Review and Editing; Project Administration; Funding Acquisition.

Declaration of interests

☐ The authors declare that they have no known competing financial interests or personal relationships that could have appeared to influence the work reported in this paper.

☒ The authors declare the following financial interests/personal relationships which may be considered as potential competing interests:

Mohamed Katish reports financial support was provided by EPSRC. Veronica Ferrandiz-Mas reports a relationship with Engineering and Physical Sciences Research Council that includes: funding grants. If there are other authors, they declare that they have no known competing financial interests or personal relationships that could have appeared to influence the work reported in this paper.